NASA CR 72376
09357-6006-R000

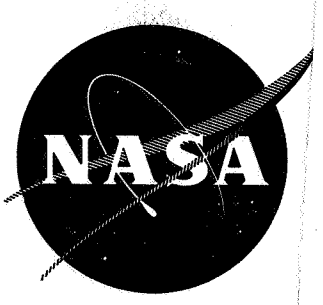

OPERATION OF SOLAR CELL ARRAYS IN DILUTE STREAMING PLASMAS

by

Robert K. Cole, H. S. Ogawa, and J. M. Sellen, Jr.

prepared for

NATIONAL AERONAUTICS AND SPACE ADMINISTRATION

CONTRACT NAS3-10612

TRW
SYSTEMS GROUP

NASA CR 72376
09357-6006-R000

FINAL REPORT

OPERATION OF SOLAR CELL ARRAYS IN DILUTE STREAMING PLASMAS

by

Robert K. Cole, H. S. Ogawa, and J. M. Sellen, Jr.

prepared for

NATIONAL AERONAUTICS AND SPACE ADMINISTRATION

March 15, 1968

CONTRACT NAS3-10612

Technical Management
NASA Lewis Research Center
Cleveland, Ohio
Space Power Systems Division
Thomas Klucher

TRW Systems
One Space Park
Redondo Beach, California

TABLE OF CONTENTS

OPERATION OF SOLAR CELL ARRAYS IN DILUTE STREAMING PLASMAS

by Robert K. Cole, H. S. Ogawa, and J. M. Sellen, Jr.

TRW Systems

SUMMARY

The operation of solar cell arrays in dilute streaming plasmas has been examined. Plasma streams generated in a plasma wind tunnel have been directed against solar cell panels. Ion mass, ion streaming velocities and plasma densities simulate, in general, conditions encountered by spacecraft orbiting in the lower ionosphere (300-500 kilometers altitude). Electron drainage currents from the plasma to the solar cell array have been determined as functions of cell bias potential and plasma density. Solar cell bias potentials have ranged from 0 to 3000 volts positive with respect to the plasma. Electron drainage currents at high cell bias potentials have enacted severe power penalties against overall cell operation. Deterioration of cell insulating material with consequent increase in electron drainage current has been observed. Electron drainage to representative drainage points with "pinhole" geometry and "slit" geometry has also been determined. Exact limits to cell potentials for continued non-deteriorative operation have not been determined. Possible operating potentials, however, are seen to increase for decreases in plasma density corresponding to increased spacecraft altitudes.

INTRODUCTION

The generation of on-board electrical power for spacecraft has relied, almost entirely, upon solar cell arrays. The available power from these arrays was initially at a modest level, and a forecast of future demands upon solar arrays would, probably, have limited the role which such devices would play as the required level of power increased. However, technical difficulties in the development of alternative means of power generation have delayed the emergence of operational systems and have revised substantially the performance levels which were predicted. The development of solar arrays, on the other hand, has benefited from several innovations which were not present when earlier forecasts were formulated. Thus, it now becomes possible to consider solar arrays as candidates for "high level" power sources, even in the multi-kilowatt range.

For solar arrays delivering power at levels of tens of kilowatts, there are questions of the most appropriate currents and voltages. If the voltages utilized are in the conventional range, then thousands of amperes may be required. This, in turn, places considerable demands upon the physical size of the conductors transporting the current. If, however, power could be delivered at levels of several thousand volts, then the power system, itself, would only be required to handle currents of the level of amperes. Beyond this, there are situations in which the power is most appropriate when delivered at high voltages because of load requirements or power conditioning requirements.

The operation of solar cells at high potentials raises a series of problems, some of these resulting from the nature of the space environment. In particular, the ambient plasmas in space possess charge carriers of both polarity and one or the other of these will drift to the high voltage portions of the solar array if leakage paths can be established. The mobility of electrons, the negative charge carriers, greatly exceeds that of the ions, so that a major concern would be raised for solar cell arrays operated at high positive potentials. Previous studies (for example, see NASA CR-54692) had

established that the level of electron drainage from the space plasma to exposed portions of low positive voltage solar cells was sufficient to create problems in the potential equilibration of the spacecraft with the plasma and that prohibitively large levels of drainage result at even modest solar cell potentials for cells operating without cover glasses. The interest of the program of research here reported was to extend these earlier findings to solar cell arrays operating at potentials in the kilovolt regime.

PROGRAM REVIEW

The first series of experiments were conducted with a silicon solar cell array of "conventional" construction in which cover glasses were in place over the cells, but the interconnecting tabs between cells were exposed and could act as drainage points. This solar array was placed in a "plasma wind tunnel" whose plasma stream simulates the particle densities that exist in the lower ionosphere and whose plasma streaming velocity is similar to the apparent plasma streaming velocity experienced by an orbiting spacecraft in its motion through the ionosphere. Positive potentials, relative to the plasma potential, were applied to the solar cell array and the electron drainage currents measured. Two major aspects of behavior were noted. The first was that the level of drainage to the interconnecting tabs alone was prohibitive at potential biases of several hundred volts, leading to power losses in the drainage flow which are comparable to the expected power generation from the solar array. The second major aspect of the observed behavior was that the electron drainage was unstable, exhibiting regularized oscillations with frequencies in the range of several kiloHertz. These fluctuating current drainages would produce severe problems in spacecraft potential equilibration with the space plasma, particularly for spacecraft with scientific payloads.

The next direction for the program was to apply an insulating sealant over the interconnecting tabs and over any further exposed areas such as those found on the solar cells at the edges of the cover glasses. The application of such a sealant had proved satisfactory in reducing equilibration

problems for the spacecraft described in NASA CR-54692. For the present program considerable care was exercised in the application of the sealant with repeated applications and cureings to assure that exposed areas were thoroughly insulated. This treated panel was then placed in the plasma wind tunnel and positive bias potentials were applied. The initial behavior of the panel was that drainage currents were well within the tolerable limits for bias potentials up to several thousand volts. However, the drainage currents did increase for continued operation in the plasma stream and, within a comparatively short interval of time, reached levels which were no longer permissible. Indeed, continued operation led to power drains considerably in excess of the power generation rate for the solar cell array. Continued operation in the laboratory was possible, in that the power losses were supplied by the supplies providing the bias potentials. In space, however, the power drainage would be limited to that provided by the solar array which would be in a state of total compromise.

The most significant aspect of the behavior noted here was the deteriorative nature of the drainage. When the solar panel was withdrawn from the plasma wind tunnel it was found that the insulation was partially or totally eroded in many places, thus providing clearly defined drainage paths for the electrons. The extent of the ablation of material had not been expected, and its discovery resulted in a major redirection of emphasis in the program of research.

The experience of the deterioration of the "insulated" solar array indicated that even minute openings were capable of providing drainage paths for electrons and that the power input to the drainage points was sufficient to cause an enlargement of the drainage path, leading eventually to a complete breakdown condition between the solar array and the streaming plasma. The further definition of the indicated process, however, would not proceed easily with such a large and comparatively complicated structure as the solar panel. Many separate, small, initial drainage points could be participating in the drainage and their geometries could be widely varying. To provide a more clearly defined problem for study, the program turned to recognizable and specified drainage path sizes and geometries. The studies with these drainage "pinholes" and "slits" confirmed that the collected

current of electrons is "anomalously" large and that the drainage power from these currents is sufficient to create the observed destruction of materials and enlargements of drainage paths. The description of the drainage as "anomalous" is used here to indicate that the current is large compared to that expected from a stationary plasma to the drainage point. The plasma incident upon the solar panel is, however, a streaming plasma since the general situation is that relative motion does exist between a spacecraft and the space plasma. For a streaming plasma it would appear that there are many factors contributing to an increase in the allowable collected current, compared to expected values for stationary plasmas. Several of these factors are discussed in greater detail in the body of the report. These considerations, taken together with the observed behavior, provide considerable insight into the behavior of the solar cell-plasma stream configuration.

Having examined the behavior of silicon solar cell arrays with and without insulating materials on the interconnecting tabs, and the behavior of definable pinholes and slits, the program turned finally to an examination of a CdS thin film solar panel. Here the panel material is totally encapsulated in the cell manufacturing process, with thin insulating layers being outermost on the several layers comprising the cell. Such a construction should prevent any electron drainage, provided that the insulating material is, indeed, free of even minute openings. However, when the solar panel was placed in the plasma stream, and when positive potential biases were applied to the panel, it was found that electrons were being collected. The initial drainage of electrons was small, similar to the behavior observed when the silicon solar panel was under test. The electron drainage to the CdS panel also increased as a function of time, eventually reaching levels of prohibitive power drainage. When the panel was removed from the chamber numerous points were observed at which minor damage had occurred, and several points of extensive charring of the insulating material were also noted.

CONCLUSIONS

The results described above comprise the major aspects of the overall program of research. From the program one may conclude that operation of solar cells at positive biases cannot proceed beyond certain limits without increasingly destructive effects on the array and its operation. These limits are not, however, clearly defined. As the density in the plasma stream is diminished, the drainage currents diminish and additional positive biases may be applied to the cell before arriving at some "threshold" for destruction. There would appear to be, thus, some "critical" potential bias which would vary as some inverse power of the plasma density. Even this loosly phrased criticality is unclear, however, since the allowable operation times before "breakdown" for an actual solar array in space greatly exceed the testing times utilized thus far in the laboratory. Finally to be considered are the conditions of manufacture for the solar panel material. The tests with the CdS array indicate that present manufacturing processes do not yield insulating covers over the cell material which are free of pinholes. By increasing the thickness of the insulating material, benefits of extra insulation would derive, at, however, a penalty of additional weight to the solar array. Yet, even the allowable initial size of a pinhole remains unknown, particularly if very extended periods of operation were demanded of the solar array. In summary, the program of research has identified problems which are crucial to the operation of high positive voltage solar arrays in the space plasma and has indicated directions for the understanding and solution of these problems.

I. SILICON SOLAR CELL TESTS PERFORMED IN AIR

The first experimental effort of the program was to determine the current-voltage (I-V) characteristics of a solar cell array without protective cover glasses ("bare" solar cells). The panel consisted of 234 silicon solar cells connected electrically in series, and arranged in a 9 × 26 matrix. This matrix covered an area of approximately 121 in^2. In preparation for the tests required in the contract, a solar simulator was fabricated and a radiation intensity monitor was investigated.

The solar simulator consisted of four Sylvania FBZ, 1000 watt, 3400°K frosted lamps which were mounted in Sylvania SGA reflectors. The lamp array was supported by a structure enabling intensity variations, and designed so that it could be conveniently placed into the 4' × 8' plasma wind tunnel. Immediately available for intensity distribution measurements was a TRW model 43A radiometer which had been previously calibrated by the Environmental Test Laboratory of TRW.

The first experiments were performed in air in order to relieve the anxieties of high cell temperatures produced by the lamps. By adjusting the lamps, the variations in radiation intensity had been reduced to less than 10% for the area covered by the solar cell panel. The panel was mounted on a 1/8 inch fiber glass insulating board and was located in a plane 34 inches from the plane of the lamps where the condition of 0.1 watt/cm^2 ("one sun") was obtained.

With the configuration described above, the I-V response of the "bare" silicon solar cells was determined. As expected, the open circuit voltage, V_o, and the short circuit current, I_s, of the solar cell array depended on the temperature of the panel. Variations in I-V curves were observed even in air. At room temperature (24°C) $V_o \approx 125$ V and $I_s \approx 50$ ma. The maximum output power, P_{max}, occurred with a load impedance of 2000Ω and had the magnitude $P_{max} = 4$ watts. As the panel temperature increased, V_o decreased, and I_s increased. Both had changed by a substantial amount. From the above tests, it became obvious that a different method of data acquisition was necessary. Previously, individual load resistors were shunted across the

solar cell output to measure the output power. Later, a much quicker method was developed and will be described in one of the following sections.

Following the initial experiments, protective cover glasses were placed over the individual solar cells. The transparent insulators are 0.006 inch thick, and are described as blue reflecting cover glasses on microsheet. The bonding resin used was Dow-Corning XR-63489. These cover glasses are of the same type used by TRW for such interplanetary vehicles as the Pioneer spacecraft. To determine the effect of reduced radiation intensity through the cover glasses, I-V characteristics were again measured. The solar cell response was, in general, similar to the response of the "bare" solar cell, however, a decrease in V_o to 100 V and a decrease in I_s to 35 ma was observed. A maximum output power of 2.5 watts was recorded for a load of 3000Ω. These last measurements were repeated with the solar cell mounted in the 4' × 8' vacuum chamber without any significant changes. Furthermore, no effect was observed on the I-V response when the solar cells were biased up to 1000 V. It should be noted that these last measurements were taken in vacuum with no incident plasma.

II. SILICON SOLAR CELL TESTS PERFORMED IN THE PLASMA WIND TUNNEL

The solar lamp structure, solar cell panel, and the Kaufman ion engine were mounted in the plasma wind tunnel as shown in Fig. 1. Not shown in the figure is the radiometer used in monitoring the light intensity during the experiments. This monitor was positioned outside the vacuum chamber on the axis of the lamp-solar cell array which is also the axis of the streaming plasma. In this configuration the monitor samples the output from each lamp through a plexiglass window and is shadowed from the ion source by the solar panel. Satisfactory performance of the radiometer was obtained with the monitor at a distance corresponding to about 0.3 sun intensity. Investigation of an RCA 1P21 photomultiplier as a monitor showed promising results; however, its use would require a very stable voltage input and temperature conditions not available. The temperature of the solar cells was measured by an iron-constantan thermocouple attached directly behind a spare Si solar cell which was mounted on a 1/8" fiber glass board similar to the solar panel. The monitor was placed in the plane of the solar cell panel at a point where the light intensity was approximately 1.0 sun. With the lamps on for a period of one minute, the temperature increased 20 centigrade degrees. It is assumed that the temperature rise of the solar cell panel is equivalent. The various probes shown in Fig. 1 are used for plasma diagnostics. The J_+ probes are 1/8" dia. Faraday cups which include an electron suppressor grid. The emissive probes are used to measure the plasma potential.

The solar cell panel was placed 30 inches from the solar simulators which were adjusted to give the intensity distribution shown in Fig. 2. This distance was chosen so that enough light would be collected by the radiometer to monitor the light intensity.

The schematic to the plasma source and solar cell testing configuration is shown in Fig. 3. Argon gas diffuses under pressure through a porous tungsten plug into the bombardment chamber. Ions produced are accelerated through the potential $V_S - V_G$ where V_S is the pulsed screen voltage and V_G is the grid voltage. The ions are decelerated to a final energy of $e(V_S - V_N)$ and are simultaneously neutralized by a hot tungsten filament. Voltages to the spreader grids provide a decrease in ion density of the plasma and supplements the beam attenuators placed downstream from the Kaufman source.

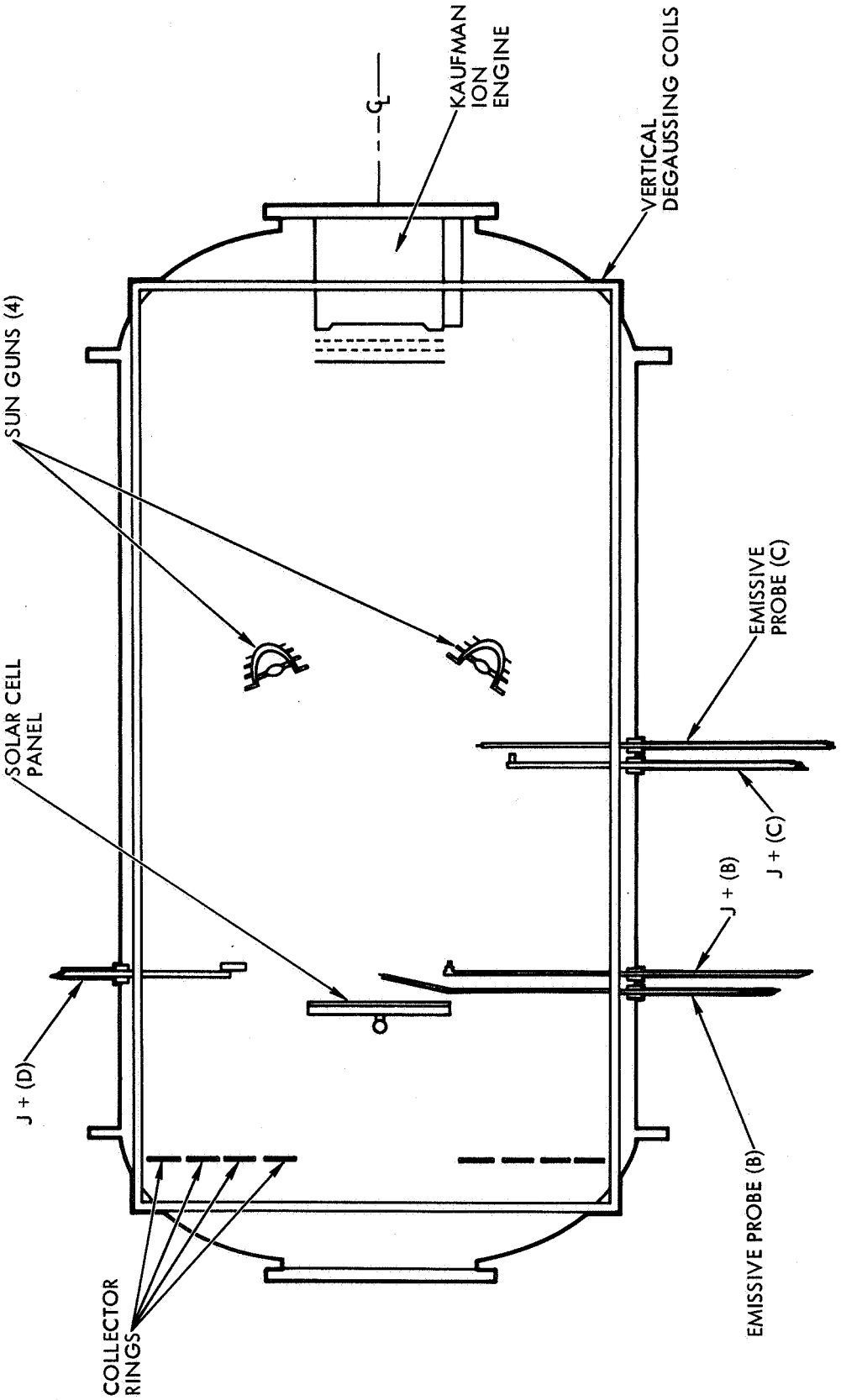

Figure 1. Experimental configuration in 4' x 8' plasma wind tunnel.

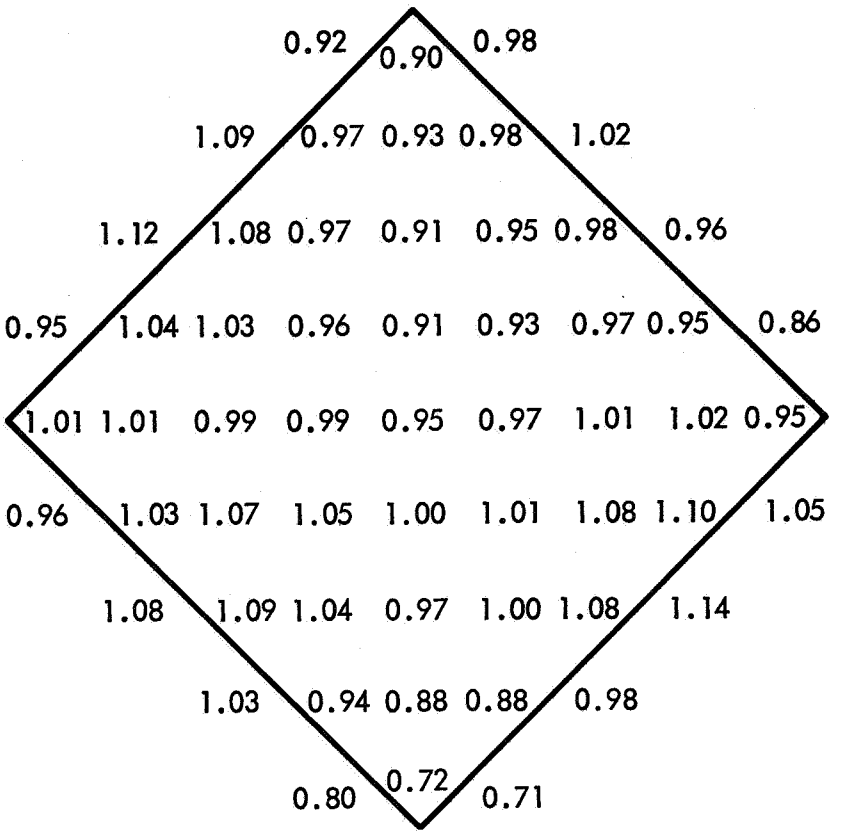

Figure 2. Distribution of radiation intensity across 121 in^2 solar cell panel. 1.00 is equivalent to one sun.

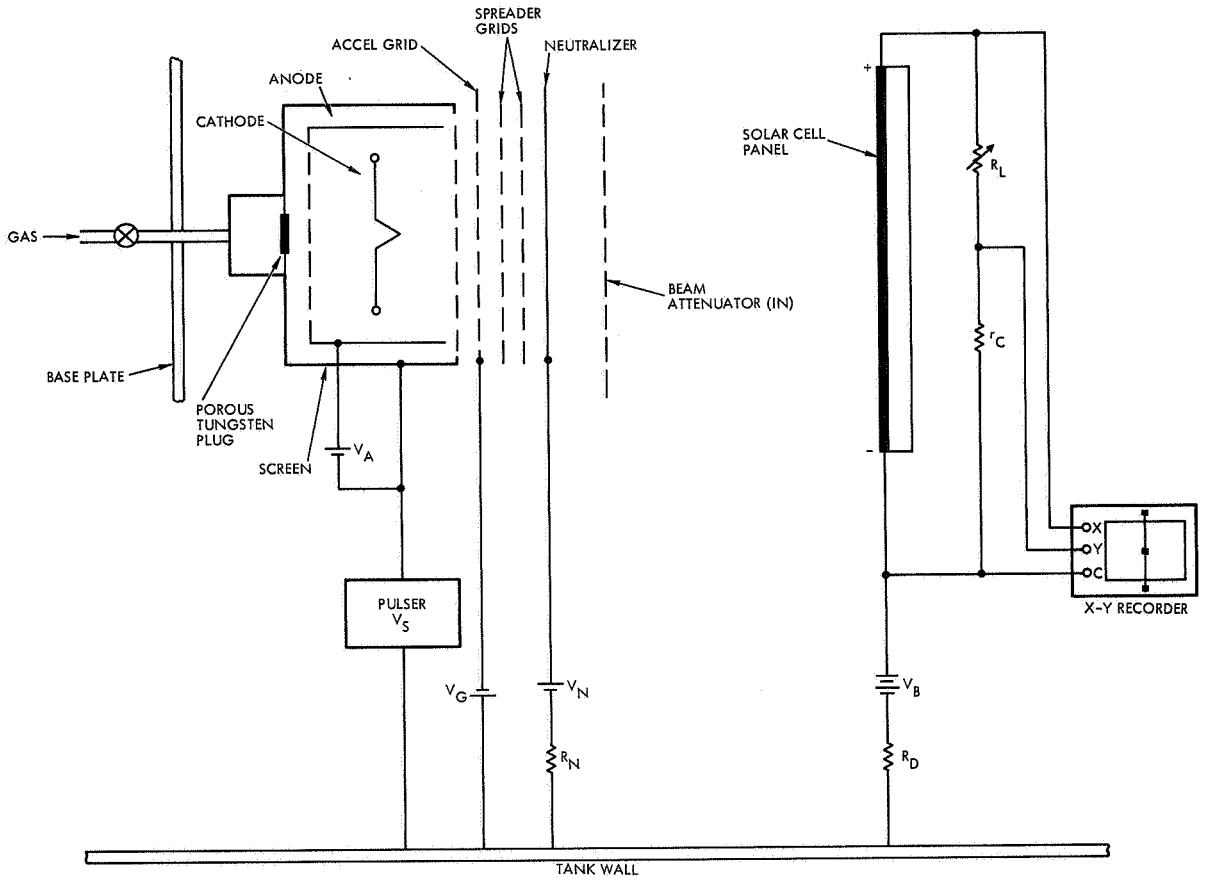

Figure 3. Schematic of experimental apparatus showing Kaufman ion engine, beam attenuator, and solar cell panel.

The neutralizer bias voltage, V_N, determines the final plasma potential. This potential is maintained positive relative to the tank walls in order to prevent plasma electrons from draining to these surfaces. The circuitry for plotting the I-V characteristic curves for the solar cell panel is also shown in Fig. 3. These curves are plotted with the x-y recorder which is at the same bias potential, V_B, as the solar cell panel. A motor driven potentiometer (10Ω to 10KΩ) serves as the variable load, R_L. The x-axis of the recorder measures the output voltage and the y-axis measures the load current by means of the potential generated across the fixed resistor r_c (0.15Ω). The motor driven potentiometer completes an I-V characteristic curve in 12 seconds, and therefore two successive curves can be obtained with about a 1% change in panel output voltage due to temperature changes. The electron drainage current, I_D, from the plasma through the solar cell panel to ground is measured by the resistor R_D. To ensure that the present circuitry did not provide any other conductance path to ground, leakage tests were performed in the absence of the plasma stream. With the lamps off, in a vacuum of 2×10^{-6} mm Hg, no leakage was observed with bias potentials up to 2500 V. Furthermore, with the lamps on, the I-V response at $V_B = 0$ and $V_B = 1000$ V were essentially overlays of each other, demonstrating the leakage currents from the panel to ground are, if anything, small compared to the currents in the load resistor. Power to the x-y recorder was provided through an isolation transformer, and precautions were made to minimize the dangers of contact with the high voltages by operating personnel.

A. SOLAR CELL CONNECTING TABS EXPOSED

The plasma density distribution for an argon beam across the solar panel is shown in Fig. 4. These measurements were obtained with the $J_+(C)$ probe located midway along the axis of the plasma wind tunnel. The beam profiles indicate a relatively uniform plasma column with very little effect due to potential biases on the solar cells. $J_+(B)$ was not used because its close proximity to the solar panel raised the possibility of accidental voltage breakdown. Because the plasma expands as it progresses through the chamber, the plasma column is even more uniform towards the rear of the chamber; however, this is accompanied with a slight loss in density.

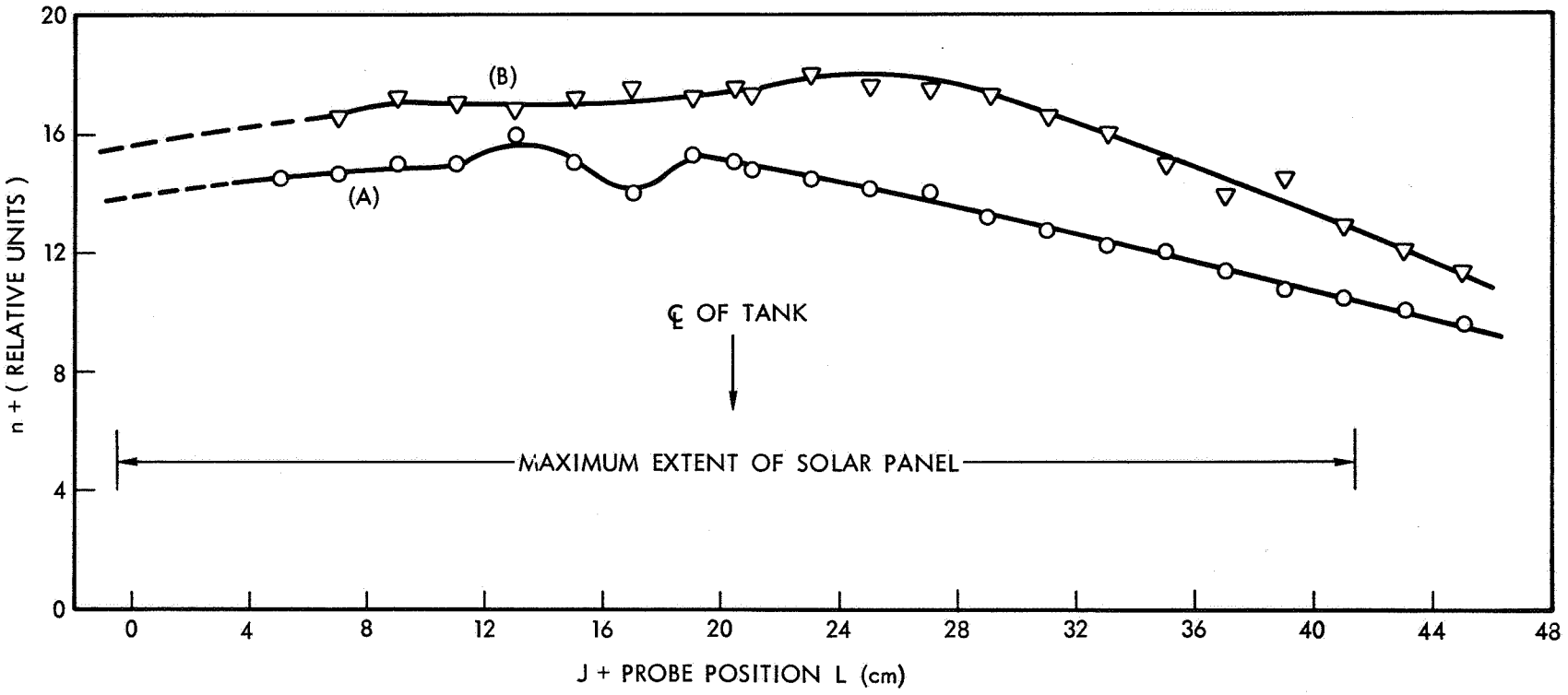

Figure 4. Density distribution of argon plasma across solar cell panel.
(A) solar panel at V_B = 0 volts; (B) solar panel at V_B = +600 volts.

The first series of experiments performed with an incident Argon plasma was the measurement of electron drainage currents as a function of solar cell bias potentials. Measurements of the I-V response were not taken, however, because of the magnitude of the drainage currents which were observed to flow to the exposed connecting tabs and edges of the solar cells. Measurements were first obtained with a plasma of density $n_+ = 7.2 \times 10^5$ ions/cm^3 and an ion streaming velocity $v_+ = 16$ Km/sec. The Earth's magnetic field was cancelled by means of degaussing coils around the vacuum chamber and the solar panel terminals were short circuited. The electron drainage current I_D plotted as a function of the solar panel bias potential V_B is presented in Fig. 5. The drainage current I_D increases approximately with $(V_B)^2$ over the range $0 \leq V_B \leq 600$ volts. The magnitude of the current was prohibitively high at this latter bias and represents about 15% of the short circuit current of the solar cells illuminated with one sun. As the bias was increased, the current collected began to oscillate at a definite frequency of approximately 5 KHz. Further increase in the bias voltage produced a sharp increase in the amplitude of the oscillations in I_D. These oscillations were also observed on the neutralizer which was supplying the electrons, the J_+ probes and the emissive probes. The behavior of the system seemed to be that of an expanding and contracting plasma column. As the bias voltage was reduced the oscillations subsisted, and a voltage much lower than the "threshold" voltage (the onset point for "large" oscillations) had to be reached before oscillations were quenched. It is speculated that this "hysteresis" effect is mostly due to changes in the conduction paths on the surface of the solar cell panel caused by local heating.

The nature of the oscillations were further studied using a Xe plasma with $n_+ = 10^5$ ions/cm^3 and $v_+ = 8$ Km/sec. Similar oscillations appeared at $V_B = 640$ V. Various parameters were varied to quench the oscillation. It was found that by limiting the electron flow to the solar cells the system would stop oscillating. This was accomplished by lowering the neutralizer temperature and also by applying a 5 gauss magnetic field transverse to the plasma flow. Other methods by which the oscillations were quenched were raising the plasma potential a few volts and increasing the ion energy.

Experiments measuring the electron drainage currents were repeated for various density argon beams ($n_+ = 0.3 \times 10^6$, 1.1×10^6, 1.9×10^6 ions/cm^3) at $v_+ = 16$ Km/sec. The results of these experiments are shown in Fig. 6.

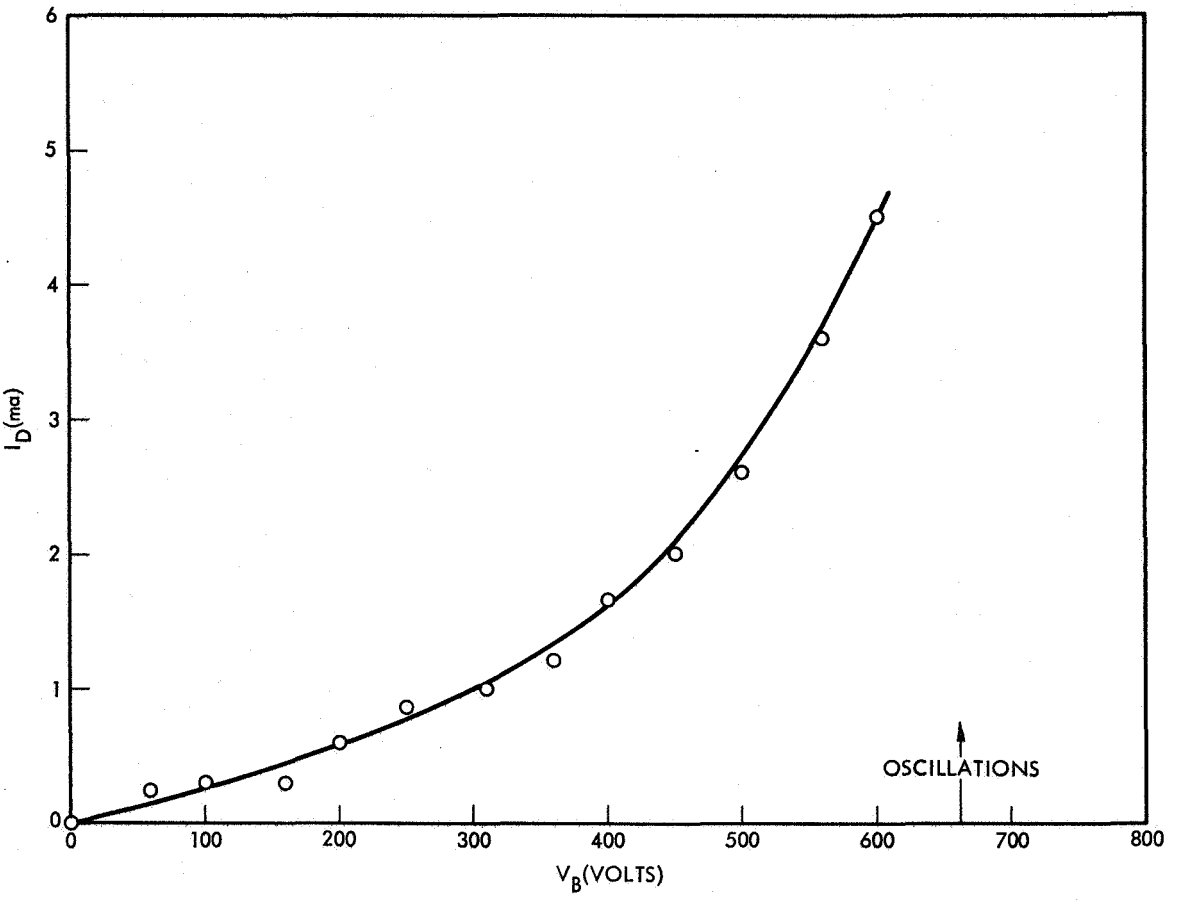

Figure 5. Silicon solar cell panel drainage current (cover glasses in place, exposed connecting tabs) as function of bias voltage. Chamber degaussed, pulsed argon plasma $n_+ = 7.3 \times 10^5$ ions/cm^3 and $v_+ = 16$ Km/sec.

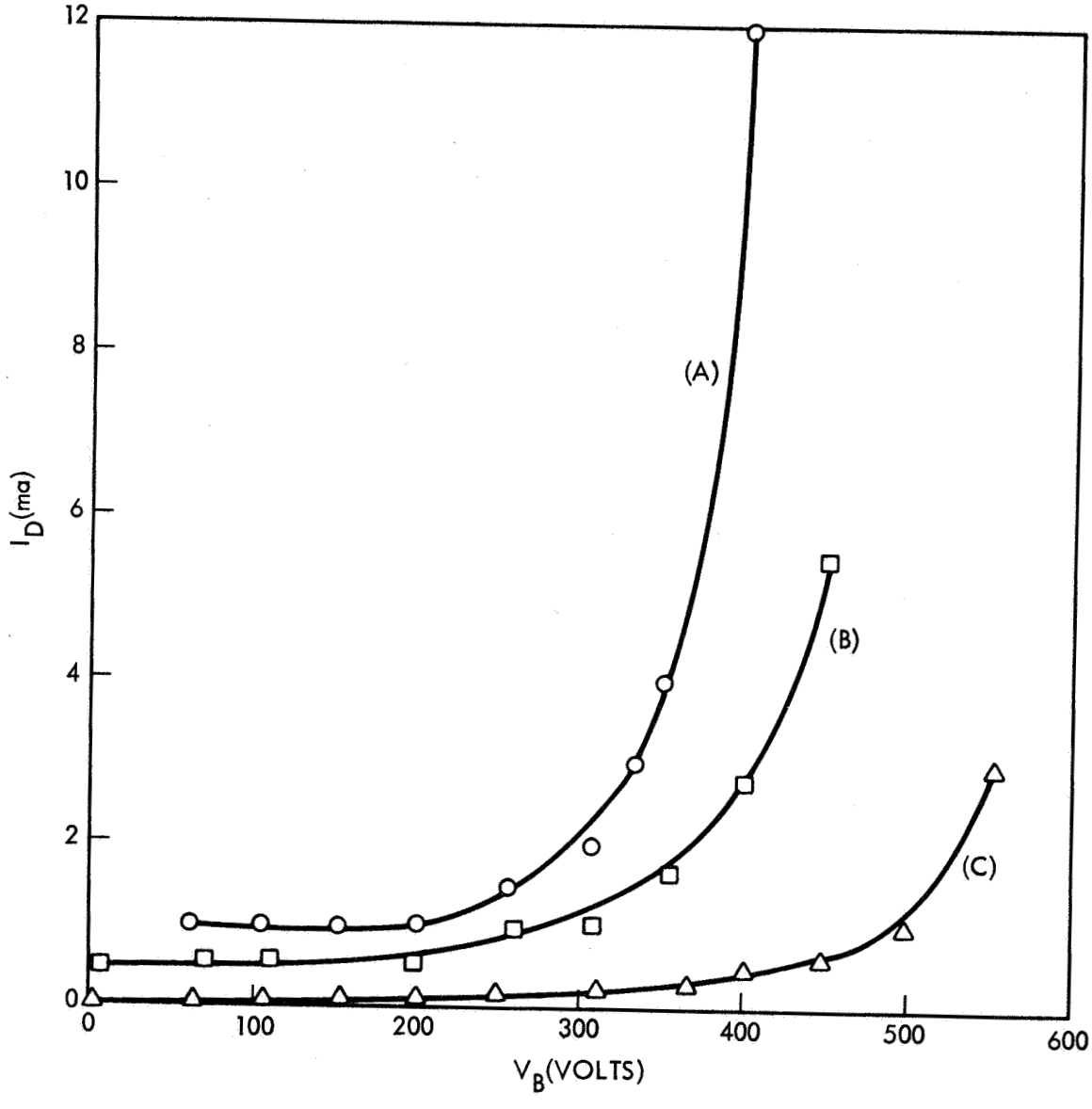

Figure 6. Silicon solar cell panel drainage current (cover glasses in place, exposed connecting tabs) as function of bias voltage V_B. Pulsed argon plasma, (A) $n_+ = 1.1 \times 10^6$ ions/cm^3, (B) 1.9×10^6 ions/cm^3, (C) $n_+ = 0.3 \times 10^6$ ions/cm^3, each with $v_+ = 16$ Km/sec.

In these experiments R_L was short circuited ($R_L = 0$) because the light intensity from the neutralizer was sufficient to produce large voltage gradients along the solar cell panel of about 40 volts. With the bias V_B applied to the negative terminal of the solar array there was no significant change in the drainage current when the shorting conductor was removed. This might be expected since the electrons normally flow internally from the positive to the negative terminal with a small internal resistance in the forward direction. All measurements of the drainage current were made with the bias applied to this negative terminal of the solar panel and with the panel short circuited. In each of the stated curves, oscillations were observed for the maximum V_B plotted. These curves show extremely high electron drainage with rapid increases for voltages above 300 V. The dependence of I_D with n_+ is not well understood in the first series of experiments. However, to get some insight of the behavior, and for convenience in comparison of the various data, a replot of Figs. 5 and 6 has been made holding V_B fixed. This set of curves is shown in Fig. 7 for V_B = 200, 300, 350 volts. The data here do show the compensating effects of sheath growth at lower densities.

B. SOLAR CELL CONNECTING TABS PAINTED WITH EPOXY

The results obtained with exposed interconnecting tabs had demonstrated that drainage currents were prohibitively high for this mode of operation. Accordingly, the exposed solar cell connecting tabs and those edges of the solar cells left exposed by the cover glass were painted with an appropriate insulator. The sealant selected was an epoxy resin (Epon 828) with a curing agent (Epon V-40) in a mixture of 50%-50%. The epoxy was carefully applied by hand and allowed to dry at room temperature for 24 hours. This procedure was repeated four times to ensure that proper insulation was achieved. The epoxy was also applied so as not to interfere with the normal light collection.

The solar cell panel was then re-positioned in the vacuum chamber and "dark" (no sun) electron drainage measurements were made with an incident argon plasma. With $R_L = 0$, $n_+ = 4.5 \times 10^5$ ions/cm^3, and $v_+ = 50$ Km/sec, the results in Fig. 8 were obtained. Comparison with the results obtained for the exposed tab condition, show a substantial decrease in the drainage

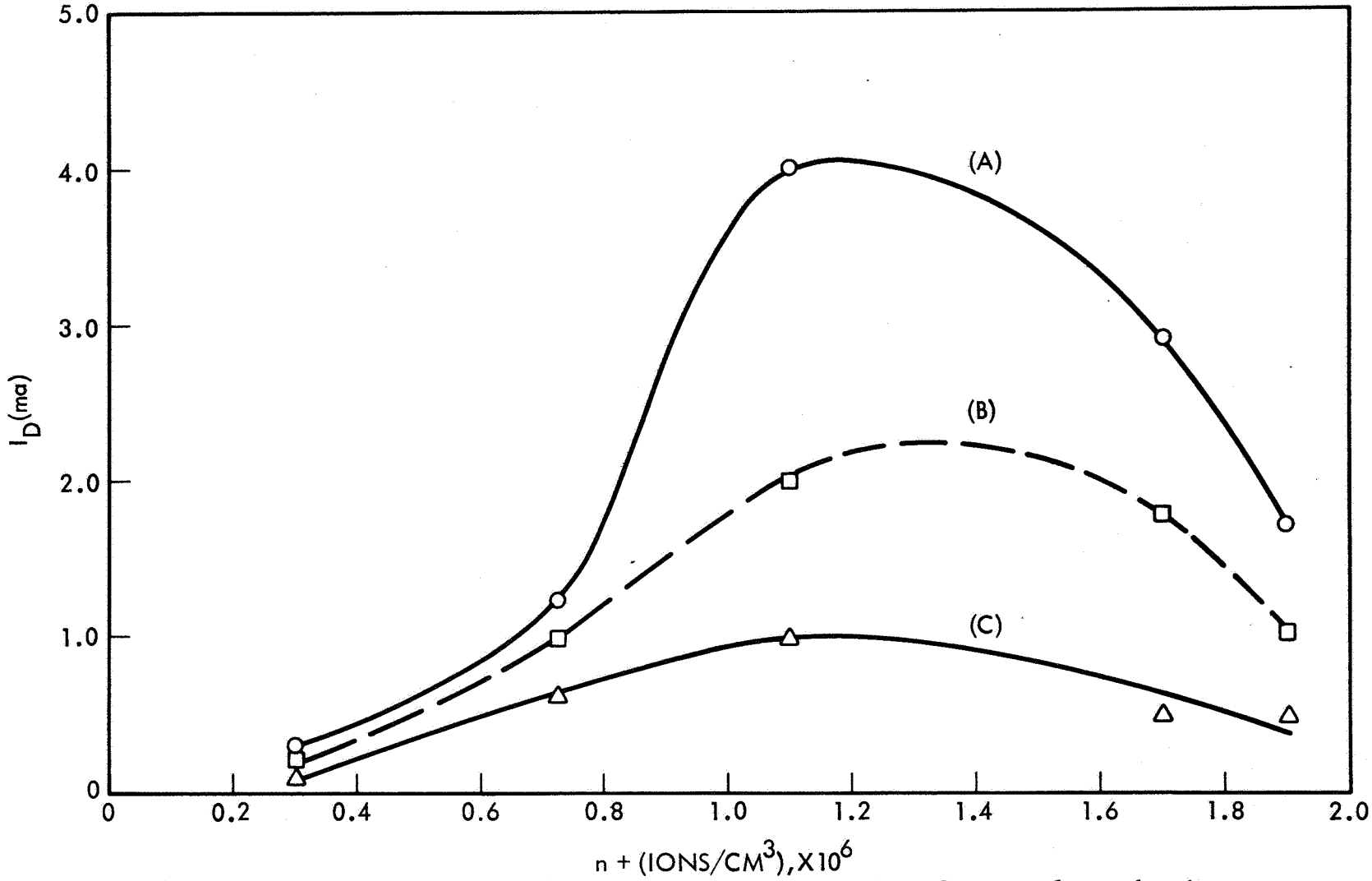

Figure 7. Silicon solar cell drainage current as function of argon plasma density for fixed panel bias voltage, (A) V_B = 350 V, (B) V_B = 300 V, (C) V_B = 200 V. (Replot of Figs. 5 and 6).

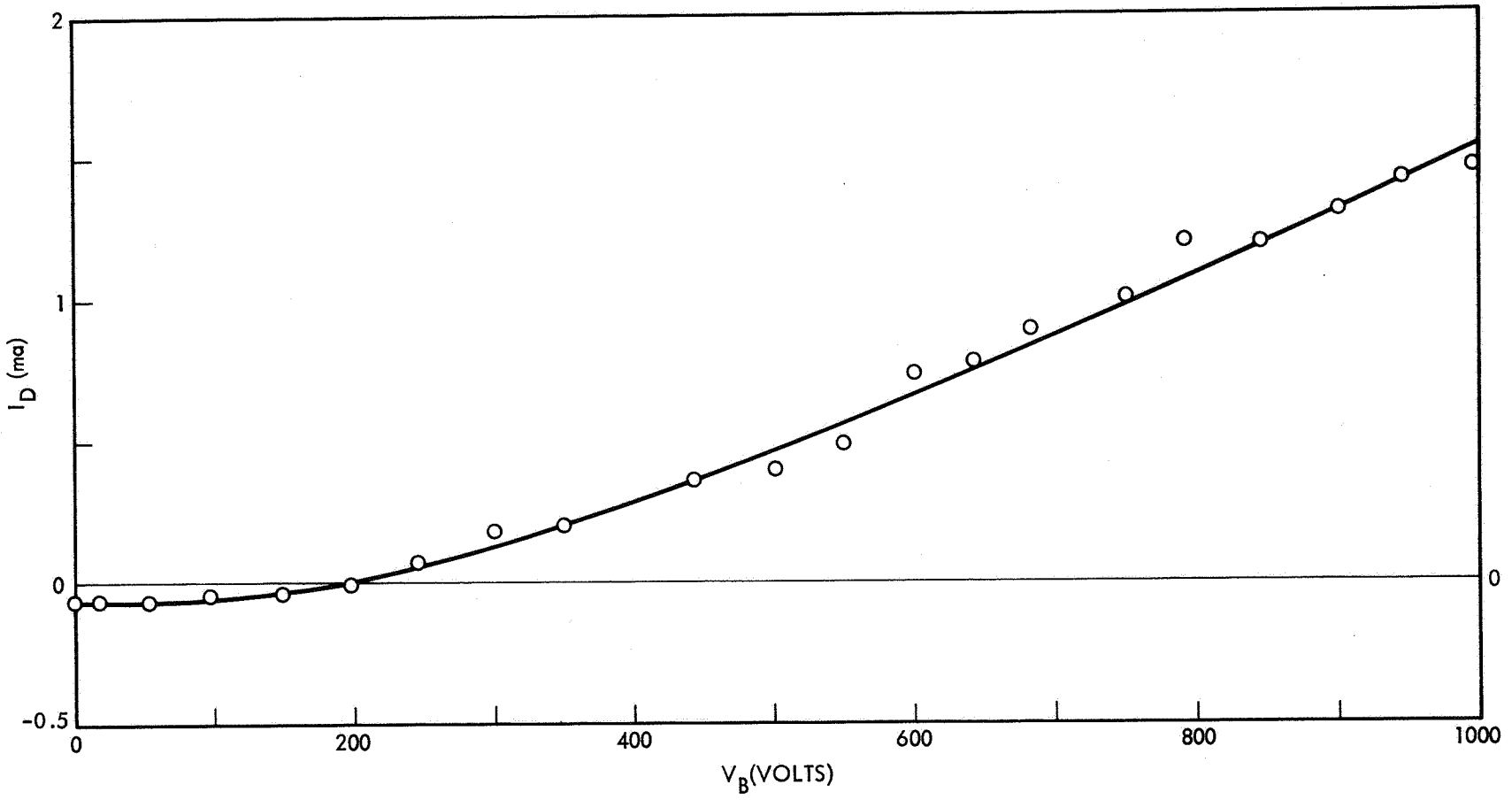

Figure 8. Silicon solar cell panel drainage current (cover glasses in place, epoxy on connecting tabs and edges of solar cells) as function of bias voltage. Pulsed argon plasma $n_+ = 4.5 \times 10^5$ ions/cm^3 and $v_+ = 50$ Km/sec.

current. Furthermore, no oscillations were observed. At V_B = 1000 V only 1.5 ma of electron drain was observed. The bias voltage was then reduced to zero and it was decided that the lower velocity incident ion beam should be applied to the solar cell panel. When the velocity was reduced to 18 Km/sec the density increased to 8×10^5 ions/cm^3. Another I_D vs. V_B curve was taken and the results are shown on Fig. 9. Apparently with this condition, sufficient drainage current was collected to break down the insulation. As shown in Fig. 9, the drainage current was substantially higher than in Fig. 8. In both cases the drainage current appeared at V_B = 200 V. However, in the latter case I_D is generally an order of magnitude higher. With the higher density, lower velocity configuration the data obtained show that as the bias voltage increased from 450 V to 500 V, a very sharp increase from 20 ma to 100 ma in the drainage current occurred. It was decided to run I-V characteristics immediately before subjecting the panel to any further damage. Holding n_+ at 8×10^5 ions/cm^3 and v_+ = 18 Km/sec, the I-V response curves shown in Fig. 10 were obtained. The data shown in this figure are replots from the data obtained from the x-y recorder at a condition of "one sun" radiation intensity and for bias voltages of V_B = 0, 195, and 410 volts respectively. The response for V_B = 195 V was similar to the zero bias response. With V_B = 410 V, the maximum output power was reduced by a factor of 2. See Fig. 11. The bias voltage was then increased to 510 V. However, the response had an erratic behavior, and very little useful power could be observed. The open circuit voltage was less than 10 V and the short circuit current less than 5 ma. These data are not shown on the figure. The electron drainage currents were not measured but should be the same as shown in Fig. 9 since the I_D vs. V_B curve was obtained just prior to the I-V characteristic measurements.

Attention then was directed on the insulation breakdown phenomena. The ion beam was turned off for several hours to permit the solar panel to cool. An argon plasma with $n_+ = 10^6$ ions/cm^3 and v_+ = 18 Km/sec was then applied to the solar cell panel. The solar cells in this case were open circuited ($R_L = \infty$). The bias voltage was varied to 2000 V and the corresponding drainage current was recorded and shown in Fig. 12. The drainage current was greater than the first measurement with the solar cell tabs painted, however, much less than the measurement where an apparent breakdown occurred.

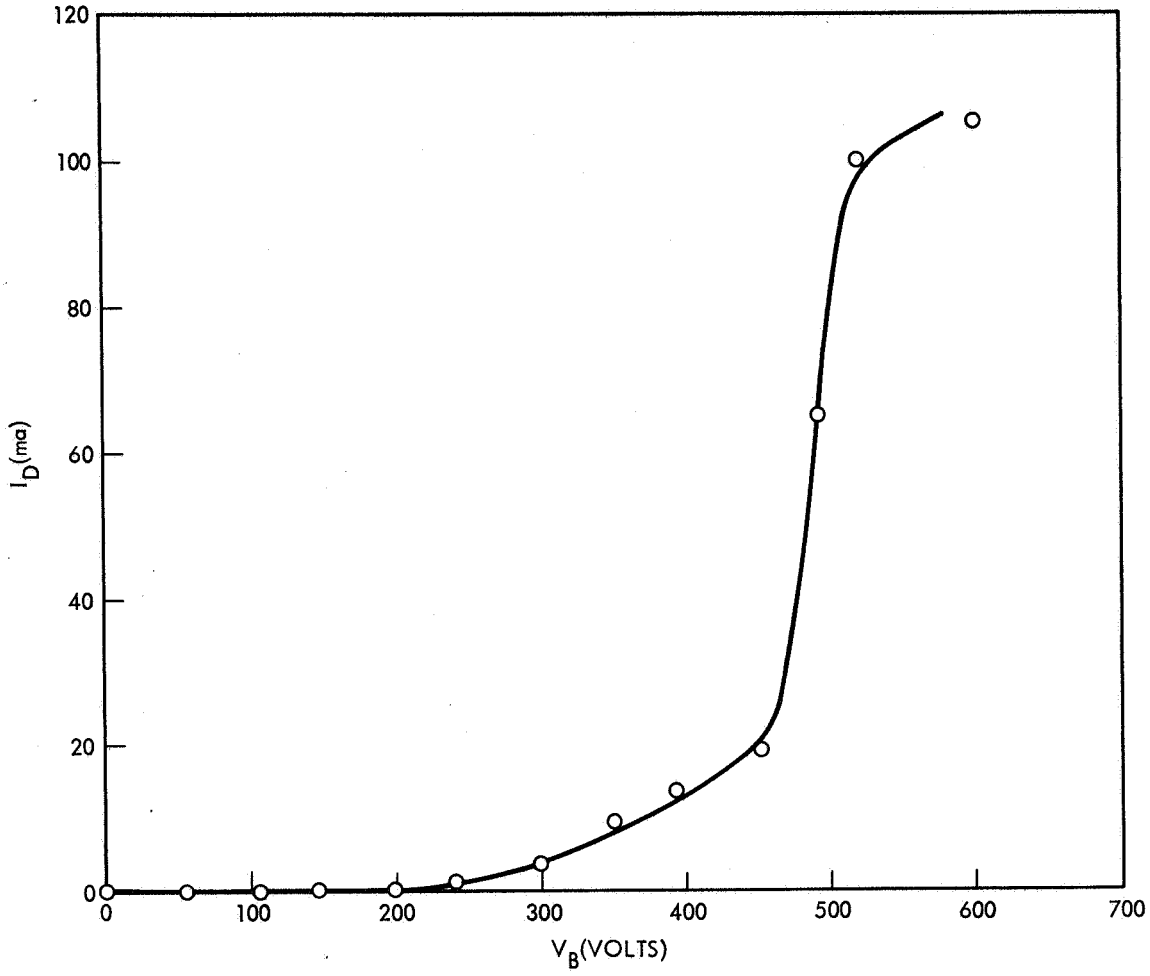

Figure 9. Silicon solar cell panel drainage current (cover glasses in place, epoxy on connecting tabs and edges of solar cells) as function of bias voltage. Effect of voltage breakdown of epoxy insulator. Pulsed argon plasma $n_+ = 8.0 \times 10^5$ ions/cm^3 and $v_+ = 18$ Km/sec.

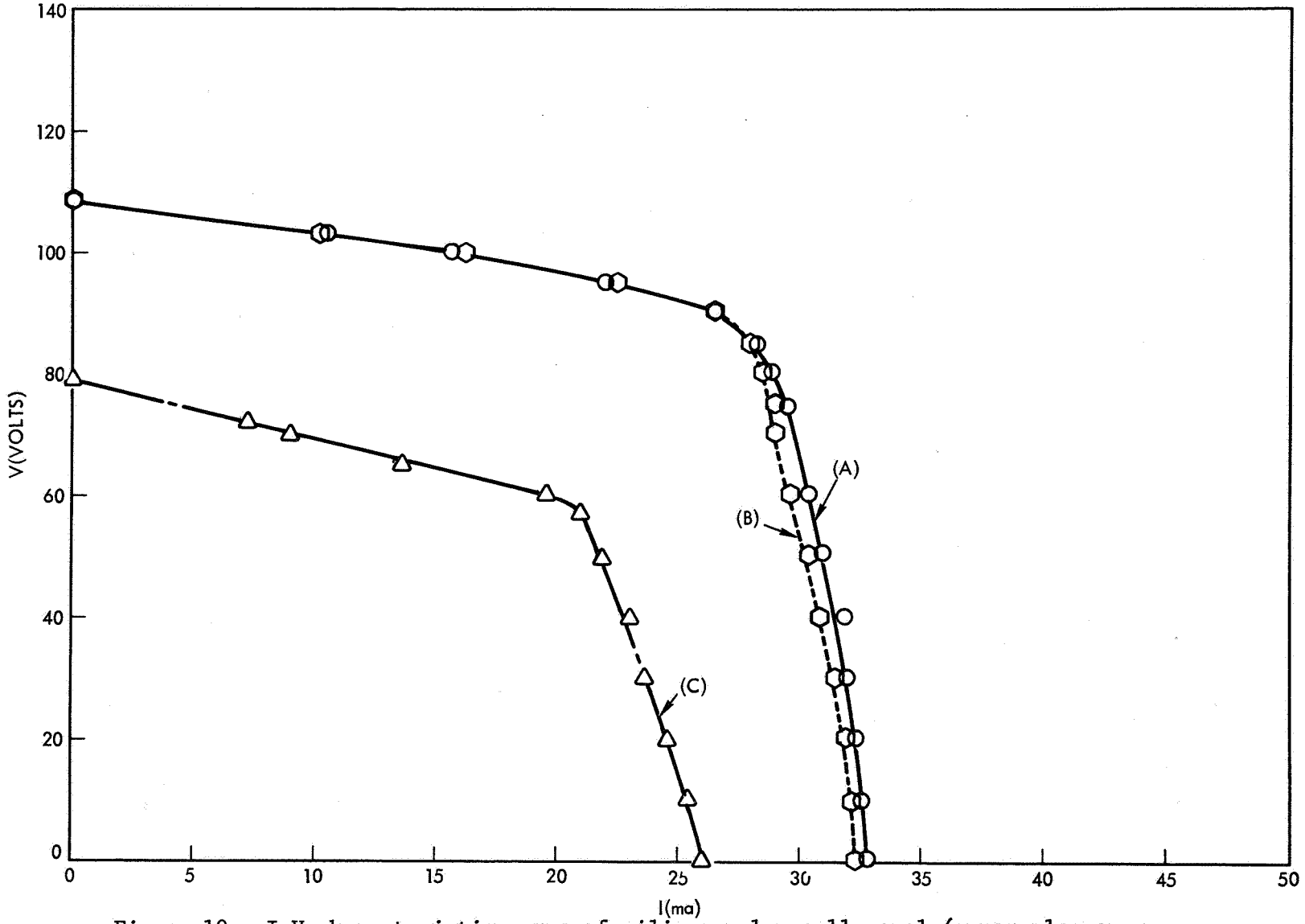

Figure 10. I-V characteristic curve of silicon solar cell panel (cover glasses in place, epoxy on connecting tabs and edges of solar cells) for bias potentials of (A) V_B = 0 volts, (B) V_B = +195 volts, (C) V_B = +410 volts. Pulsed argon plasma $n_+ = 8.0 \times 10^5$ ions/cm^3 and v_+ = 18 Km/sec.

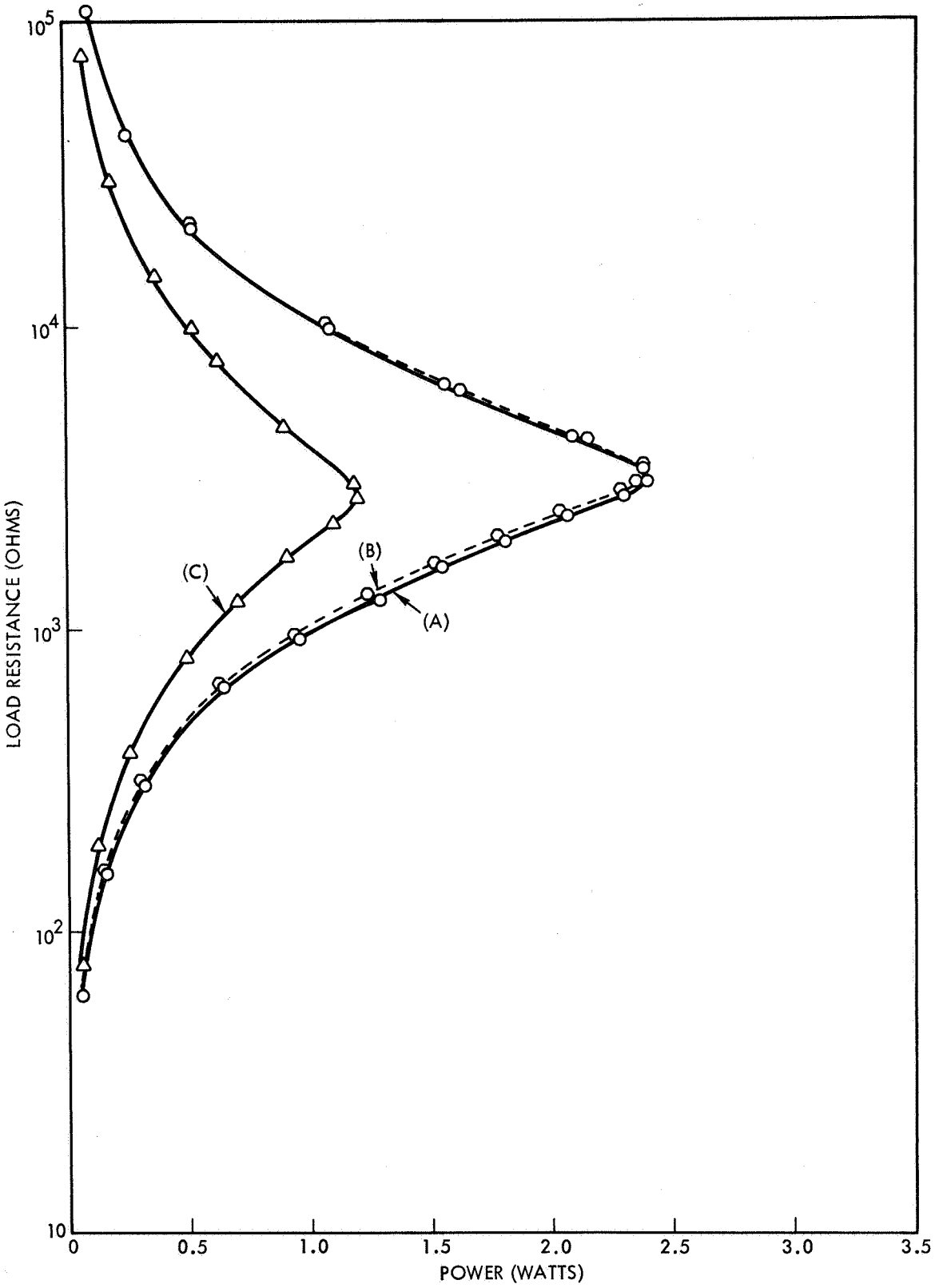

Figure 11. Silicon solar cell panel output power as function of load resistance (cover glasses in place, epoxy on connecting tabs and edges of solar cells) for bias voltage of (A) V_B = 0 volts, (B) V_B = +195 volts, and (C) V_B = +410 volts. Pulsed argon plasma $n_+ = 8.0 \times 10^5$ ions/cm^3 and v_+ = 18 Km/sec.

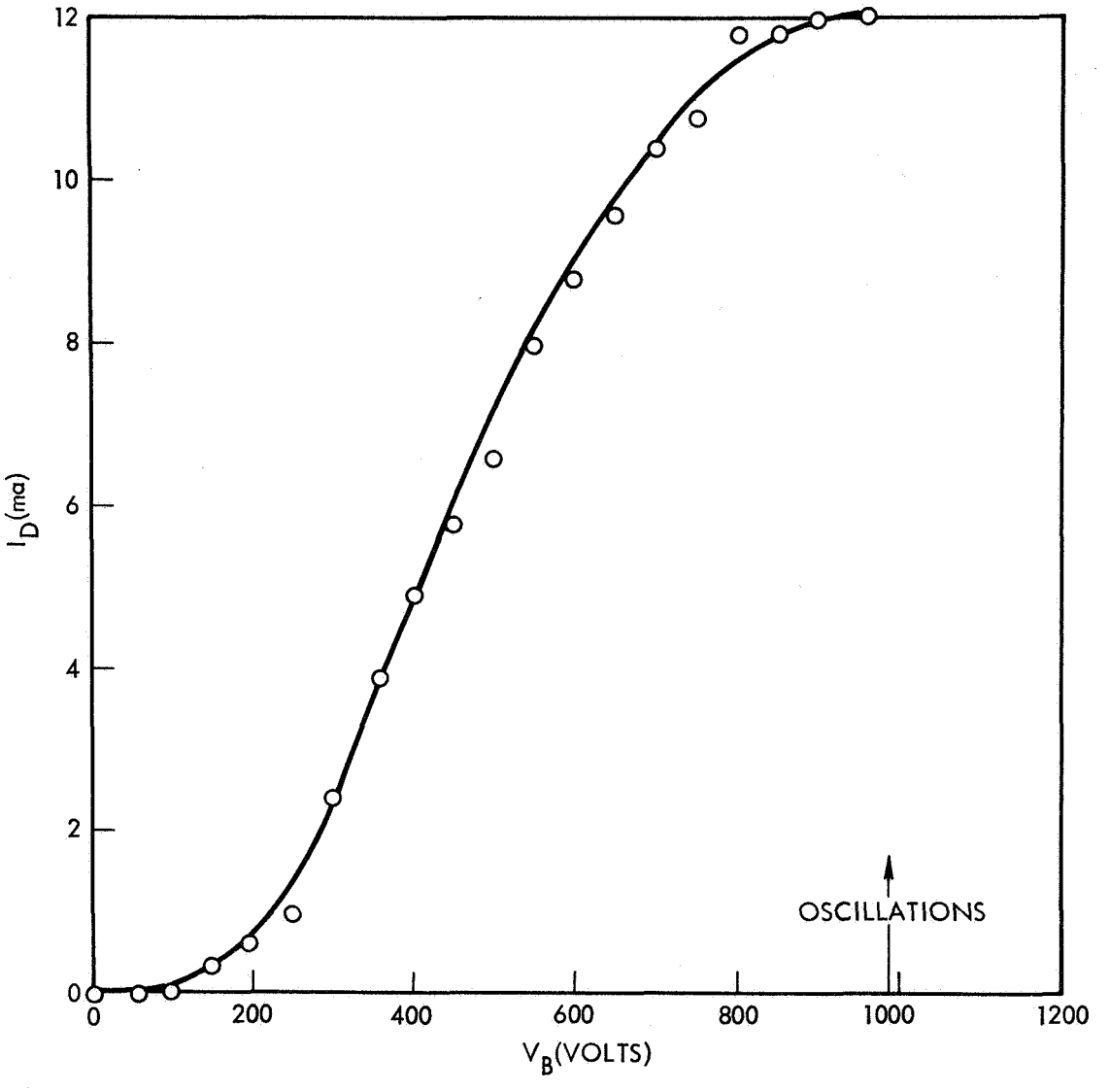

Figure 12. Silicon solar cell drainage current (cover glasses in place, epoxy on connecting tabs and edges of solar cells) as function of bias voltage following initial breakdown of epoxy insulation. Pulsed argon plasma $n_+ = 1.1 \times 10^6$ ions/cm^3 and $v_+ = 18$ Km/sec.

For bias voltages above 1000 V small oscillations were observed. The amplitudes were by no means as large or dramatic as in the case for which the solar cell tabs were exposed; however, the frequency was approximately the same. The bias voltage was held at 2000 V, and as time progressed the drainage current was seen to increase until a sharp breakdown again occurred. This time the current was large enough to blow the protection fuse of the bias power supply which was rated at 500 ma. After the bias was off for 10 minutes the 2000 V condition was re-established. The drainage current re-established at 40 ma and was increasing with time. During this run, light flashes were visible at various points over the solar cell panel, and what appeared to be a steady state discharge could be seen. The panel was then removed from the chamber and examined. Considerable damage to the epoxy insulation was found, and at a few places the epoxy had "bubbled" as can be seen in the photographs in Fig. 13. A closer examination revealed larger conducting points and pinholes which were not present before the test. Presumably, very tiny exposed points were present, and prolonged testing produced enough heating to ablate the material. The removal of material could then cause high pressure regions near the conduction points and consequently cause local discharges. It must be noted that the solar cell panel surface contains many unknown conduction points with varied geometries, and therefore only a qualitative understanding can be obtained.

At this time it was decided that experiments be conducted using simulated cells. This served two advantages. First, experiments could be performed without the risk of damaging the solar cell panel, and second, experiments could be performed with conducting samples of known geometry and describable conduction paths.

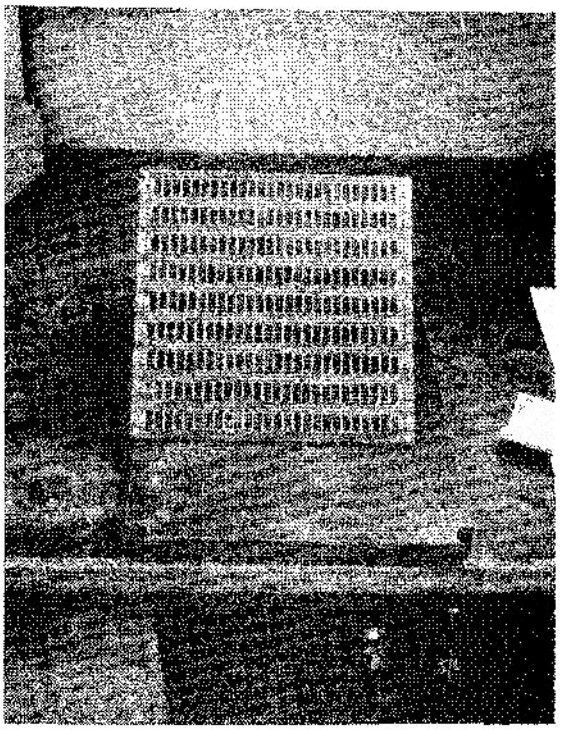

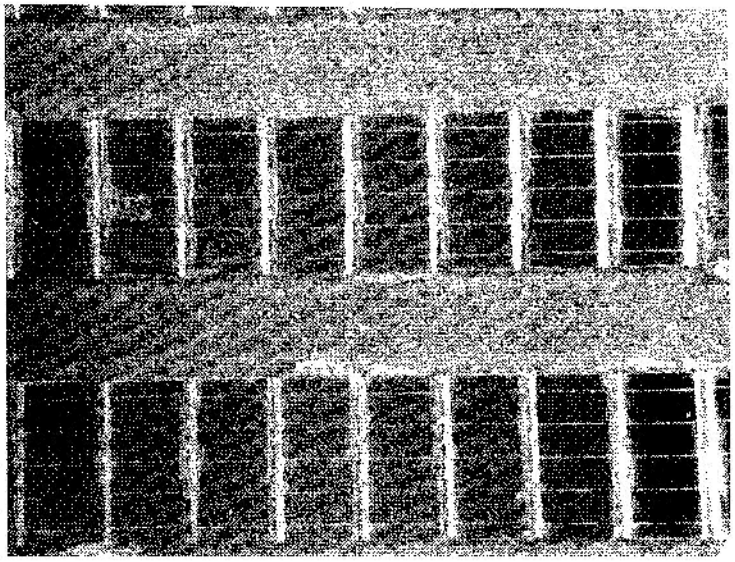

Figure 13. Silicon solar cell panel after exposure to pulsed argon plasma with high bias potentials. "Bubbles" and holes were produced in epoxy insulation.

III. CONDUCTING SAMPLES OF KNOWN GEOMETRIES CONSTRUCTED WITH DESCRIBABLE CONDUCTION PATHS

Difficulty in interpreting the data obtained with the solar cell panel led to construction of conducting samples with known surface area, shape, and conductance path.

The first of these samples (Sample A) was an Al strip 0.50 inch × 0.70 inch covered with a 0.050 inch coating of the same epoxy used to insulate the solar cell connecting tabs. The first test performed was to determine whether any conducting paths were present in the sample. Sample A was mounted on the axis of the plasma wind tunnel at the plane where the solar cell panel had been formerly placed. An argon plasma beam was applied and the sample was biased to 2000 V. No leakage was found. The sun lamps were then applied and the sample was allowed to increase in temperature to 100°C. When it was satisfied that no leakage paths were present, the sample was removed from the chamber and a hole of 0.010 inch diameter was drilled through the epoxy coating to expose the conducting surface. The photograph in Fig. 14a shows Sample A before the pinhole had been drilled with the solar cell panel in the background to give perspective. The photograph shown in Fig. 14b is a .010 inch diameter pinhole magnified by 200. Both pictures were taken before an incident plasma had been applied to the sample. Sample A was positioned in the chamber and electron drainage experiments were performed with an argon plasma of $n_+ = 1 \times 10^6$ ions/cm^3 and $v_+ = 16$ Km/sec. Initially, the electron drainage current measured less than 0.1 ma as the sample was biased to 2000 V. With prolonged exposure at high bias potentials, a growth in drainage currents along with some damage around the pinhole was observed. The sample was tested for 4 1/2 hours running time with several parameters varied so that some understanding of the behavior of the interaction between the sample and the incident plasma streams could be attained. After the initial measurement of the electron drainage had been taken, temperature effects due to the heat generated by the solar simulator were examined. Without the lamps a temperature of approximately 40°C was measured at the plane of the sample. This temperature is primarily due to the radiation from the engine neutralizer. With the bias potential of 1000 V, the sun lamps were turned

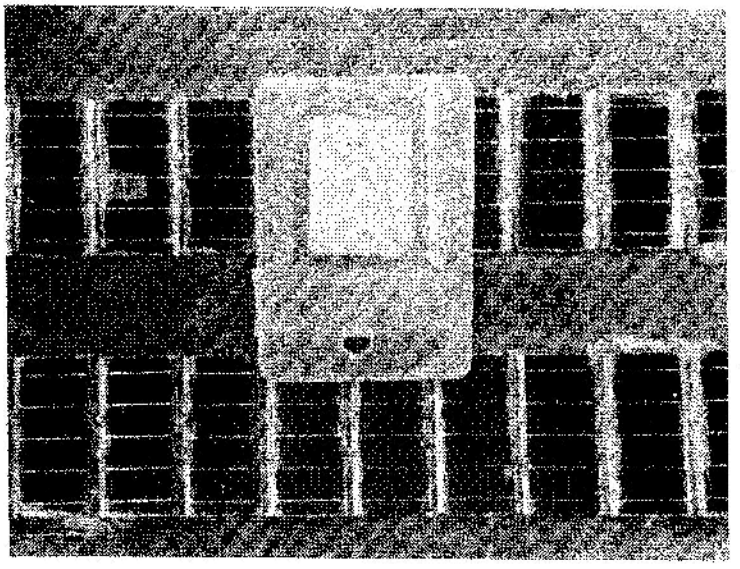

Figure 14a. Sample A without pinhole with solar cell array in background.

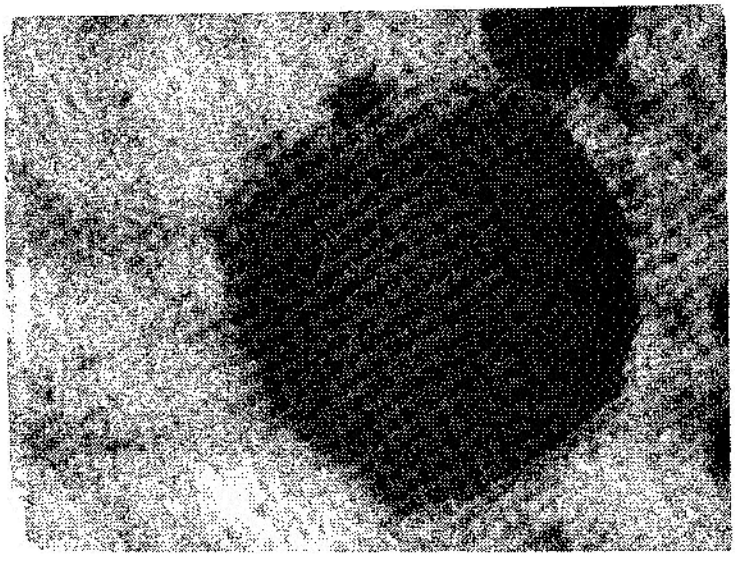

Figure 14b. Sample A with 0.010 inch pinhole drilled (X200 magnification). Both photographs taken before tests were performed.

on for 1 minute and temperatures increased to 60°C. No increase was observed in the drainage current which remained less than 0.1 ma. The sun lamps were turned off, the bias voltage was maintained at 1000 V and after 20 minutes the sample cooled to 45°C. At this time a small breakdown in the epoxy occurred. The electron drainage current increased to 0.2 ma. The bias voltage was then increased to 2000 V and the drainage current increased to 1 ma. This bias voltage was maintained for 1 1/4 hours, and during this period the electron collection increased to 2.3 ma. The sun lamps were again turned on until the sample's temperature increased to 70°C and again this had no effect on the current collected by the sample. The plasma was reduced to $n_+ = 7 \times 10^5$ ions/cm^3, v_+ was held fixed, and the electron current consequently diminished to 1.25 ma. This is indicative but by no means proof that the drainage current is somehow proportional to the density. At this density the drainage current remained relatively constant for 1 1/2 hours. The next test was to see what effect an increase in ion energy had on the electron drainage current. As the ion streaming velocity was increased from 16 to 52 Km/sec the density changed to $n_+ = 1.4 \times 10^6$ ions/cm^3. The change in volocity corresponds to a change in energy from 50 ev to 550 ev ions. The drainage current when 2000 V bias was applied to the sample increased to 4 ma which is more than a factor of 3 higher than was previously obtained. It must be noted then that some of the increase may be due to the increase in plasma density. The bias voltage was then increased to 2800 V at which point a glowing discharge was observed in the pinhole. The drainage current at this time was 4.5 ma. The ion energy was reduced again to 50 ev, and the I_D vs. V_B curve shown in Fig. 15 was taken. The drainage currents were slightly larger than those that were obtained before the high energy ions were applied. After this test the sample was removed from the chamber and examined. The hole did not appear larger; however, close examination revealed erosion around the edge of the pinhole and a slight elongation. Fig. 16a gives an overall view of sample A and clearly shows the charring around the pinhole. Fig. 16b shows the pinhole with 200 magnification.

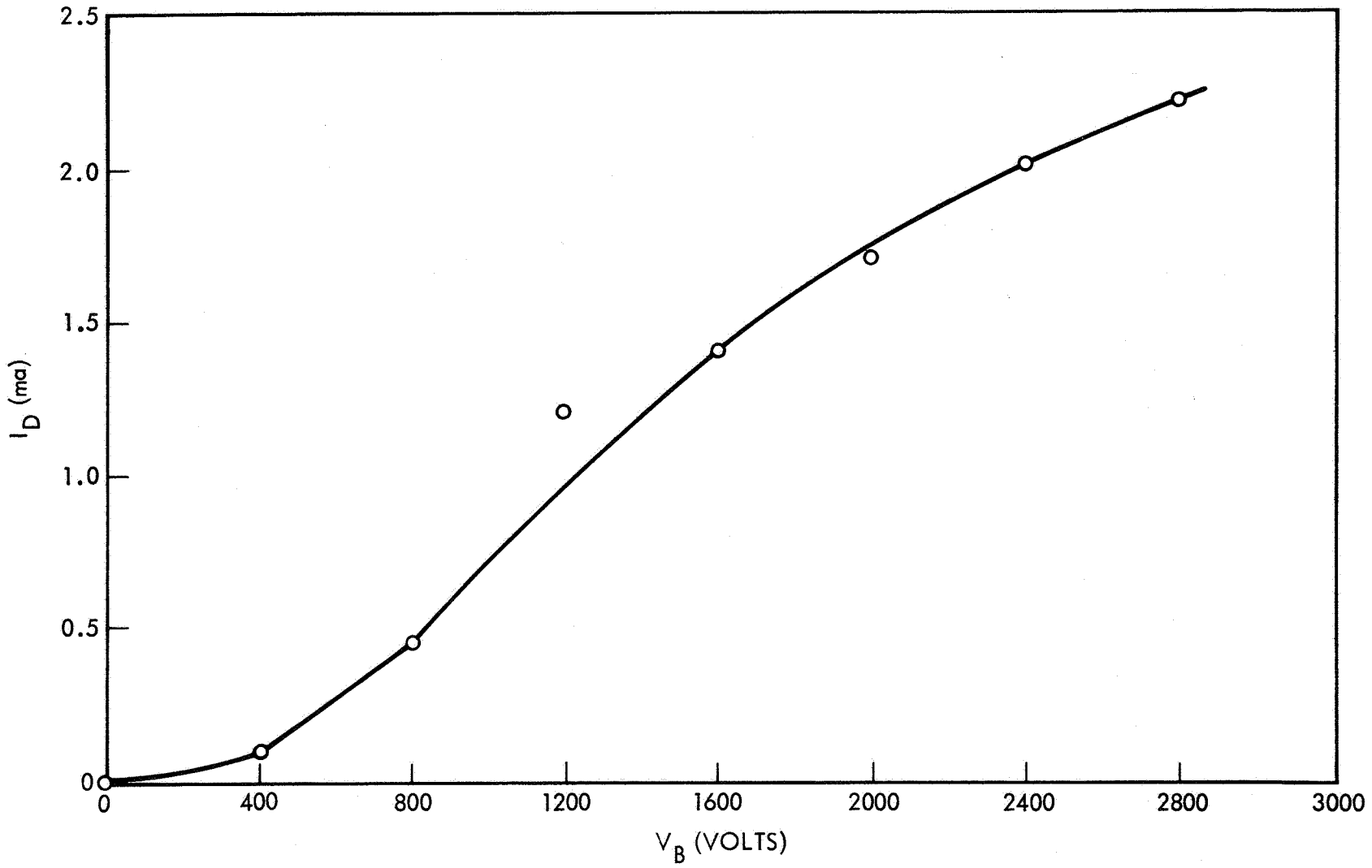

Figure 15. Drainage current of Sample A as function of bias voltage after initial breakdown in epoxy. Pulsed argon plasma $n_+ = 7 \times 10^5$ ions/cm^3 and $v_+ = 16$ Km/sec.

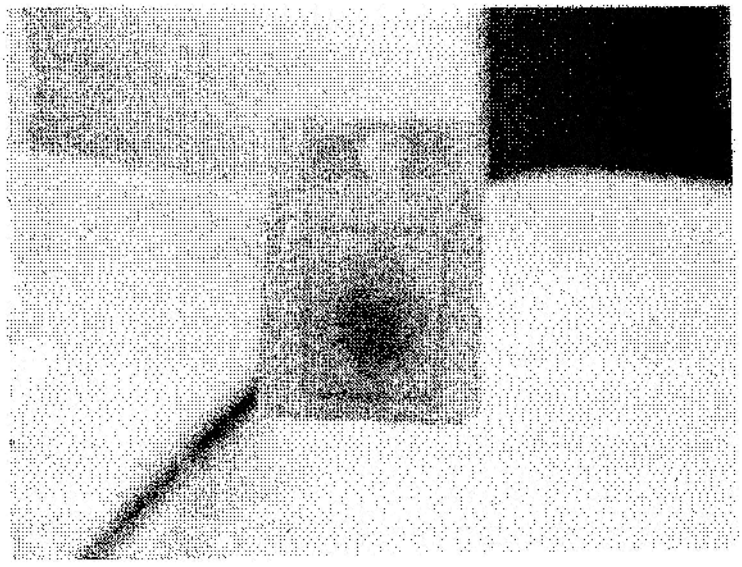

Figure 16a. Overall view of Sample A shows charring about the pinhole.

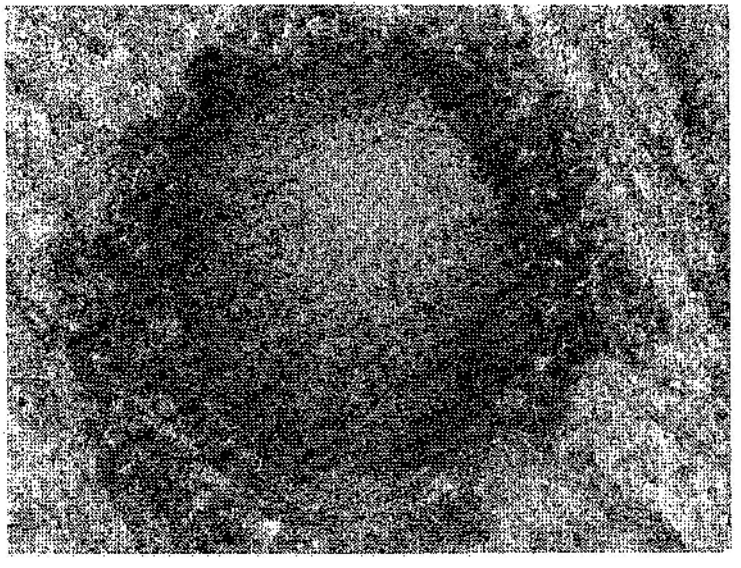

Figure 16b. Pinhole of Sample A after initial exposure (X200 magnification).

Sample A was then replaced into the chamber and again exposed to an incident argon plasma of $n_+ = 2 \times 10^5$ ions/cm^3 and $v_+ = 16$ Km/sec. With the sample biased +3000 V, less than 0.1 ma of electron current was collected. After a short while the pinhole began to glow as before. At this point the drainage current sharply increased. The bias voltage was immediately shut off. Then the bias was re-applied slowly. The glow discharge occured this time at $V_B = 1400$ V, with $I_D = 0.8$ ma. The bias voltage was reduced to zero and then increased again slowly. This time at $V_B = 800$ V three distinct spots of light were seen to glow around the edges of the pinhole. In order to determine the effects for negative bias voltages on the sample, the polarity was reversed and $V_B = -3000$ V was applied to Sample A. No current of substantive amplitude was collected by the sample with negative bias. The sample was then removed and re-examined under X20 magnification. The photograph in Fig. 17 shows that the pinhole had increased in diameter from 0.010 inch to 0.050 inch. Furthermore, the figure also shows some apparent removal of metal which is deposited on the surface of the sample.

From the above experiments, some general statements can be made. The heat generated by the radiation of the solar simulator (0.1 watt/cm^2) is small compared to the local heating produced in the pinhole when the sample collects plasma electrons. For example, 0.1 ma at $V_B = 2500$ V gives 1/4 watt of power which is concentrated in an area of 5×10^{-4} cm^2 (0.010 inch diameter hole) or 500 watts/cm^2. Furthermore, since such high power is concentrated in a pinhole, the heating could cause the epoxy to evaporate near the conducting region, and raise the local pressure many orders of magnitude. With these conditions, a discharge in the pinhole is very likely to occur if the sample is at a high enough bias voltage. When the high bias voltages are shut off, the material around the pinhole can flow into the pinhole and very rapidly cool. Therefore, consecutive electron drainage measurements at the same conditions will not necessarily produce identical results. Under prolonged testing the size of the pinhole will increase because of ablation with possible increase in electron collection. Furthermore, because the local temperature can be extremely high, the conducting element itself may melt and deposit on the surface producing other conduction paths for the plasma electrons.

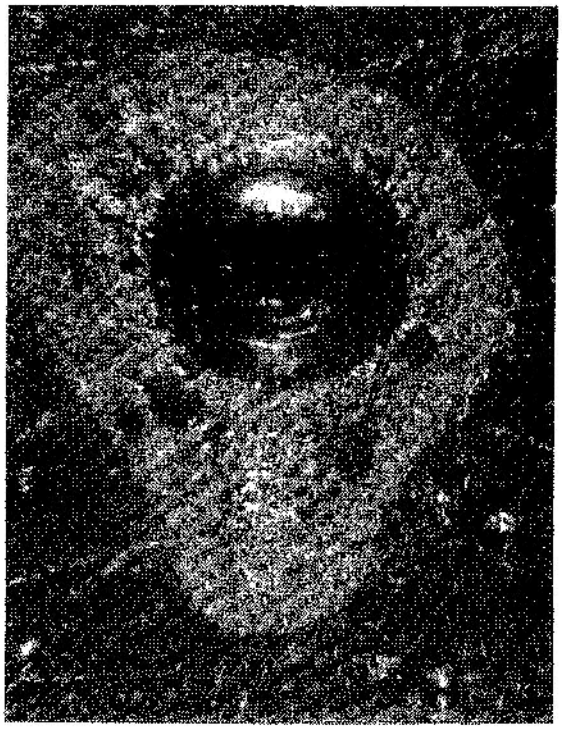

Figure 17. Pinhole of Sample A after completion of tests. Pinhole has increased in size from 0.010 inch to 0.050 inch shown with X20 magnification. Apparent Al deposited on surface of epoxy.

The second sample (Sample B) placed into the plasma wind tunnel was an exposed knife edge simulating the exposed edge of the solar cell (which is not covered by a conventional cover glass). The knife edge was made by embedding an Al strip 1 cm × 2 cm × 0.0063 cm in epoxy and machining the end flat to expose an Al edge 1 cm × 0.0063 cm. A relatively high plasma density of approximately $n_+ = 2.6 \times 10^6$ ions/cm^3 and streaming ion velocity of $v_+ = 16$ Km/sec was applied. The initial I_D vs. V_B curve is shown in Fig. 18. The drainage current, when compared to the pinhole experiment, is about the same. However, care must be taken in interpreting this result because the geometry of the two cases are different. Furthermore, in considering particular trajectories of electrons to the conducting surfaces, one can see differences in the two cases. With Sample A the electrons must funnel to a point and with Sample B the electrons enter into a slit. In the latter case electrons will funnel not only to a point but to many points; consequently, power will not be concentrated as in Sample A. With prolonged testing of Sample B some deterioration of the insulating material was observed. There were small increases in drainage current with time and a slight glow appeared at the end of the strip.

The next sample tested was a tantalum wire imbedded in epoxy with the front surface machined flat to expose the 0.010 inch diameter conducting wire, Sample C_1. This sample differs from Sample A in that the conducting element is flush with the epoxy surface rather than at the bottom of a 0.010 inch diameter pinhole. The sample was placed in the plasma wind tunnel, and initially only a drainage current of 0.1 ma was observed as the wire was biased to $V_B = 2600$ V with a plasma density of $n_+ = 4.7 \times 10^5$ ions/cm^3 and $v_+ = 16$ Km/sec. The power concentrated at the end of the wire was about 500 watts/cm^2. The drainage current increased with time. A plot of I_D vs. V_B is shown in Fig. 19. At the conclusion of this measurement a sharp breakdown occurred at $V_B = 2900$ V and light was observed at the conducting point. The bias voltage was reduced to 2500 V at which point the drainage current was 1.5 ma. Bright spots were then seen on the surface of the epoxy; however, the conducting point was dark. After the test, the sample was examined under a X30 magnification and it was observed that the 0.010 inch diameter Tantalum wire had been removed to a depth of approximately 0.05 inch. The hole

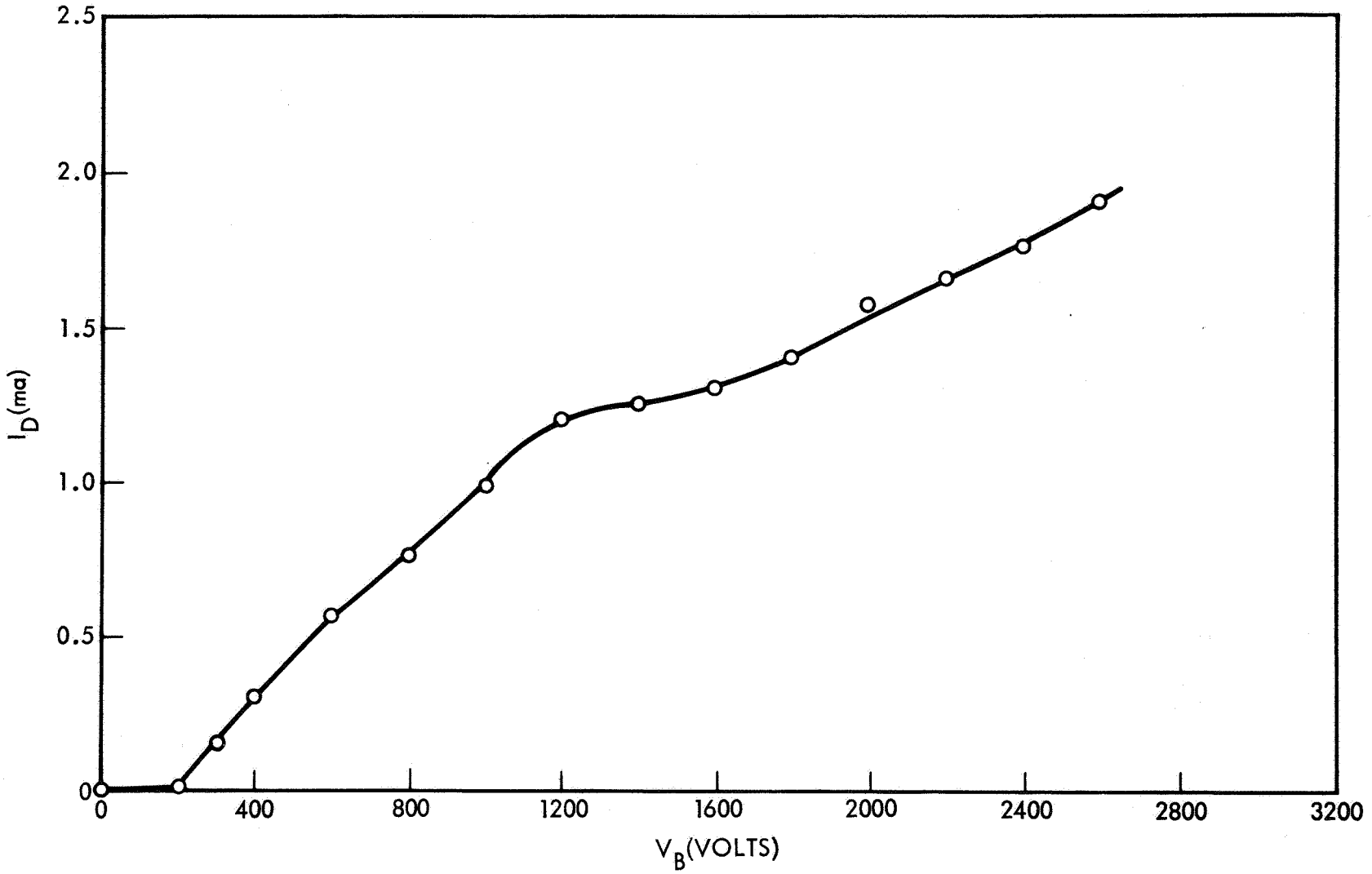

Figure 18. Drainage current of Sample B as function of bias voltage pulsed argon plasma $n_+ = 2.6 \times 10^6$ ions/cm^3 and $v_+ = 16$ Km/sec.

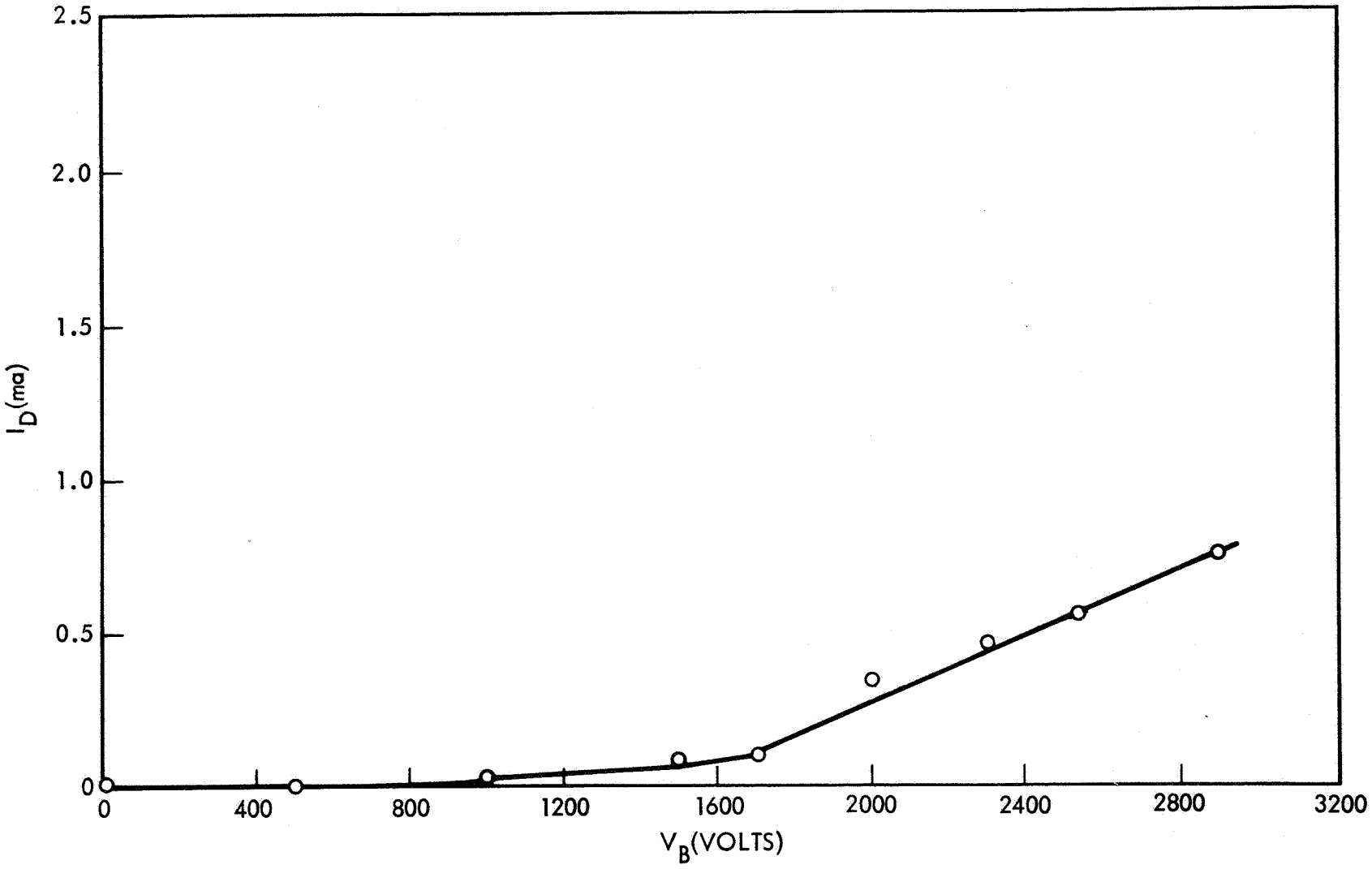

Figure 19. Drainage current of Sample C_1 as function of bias voltage just prior to major breakdown. Pulsed argon plasma $n_+ = 4.7 \times 10^5$ ions/cm^3 and $v_+ = 16$ Km/sec.

produced was irregular in shape and it appeared that sputtered Ta had collected on the surface of the epoxy apparently increasing the area of the conduction paths to the 0.010 inch wire. It is difficult to assume that the electrons could sputter the metallic surface of Ta, and therefore it is believed that the intense heat produced by the collection of the electrons at these high potentials and the concentration of power in a small area was able to melt the Tantalum wire (3460°K melting point).

Following these experiments another sample (Sample D) was made in order to determine what differences might be exhibited between a Kapton insulating tape (H-film) and the epoxy. Sample D was made with a piece of stainless steel (3/8 inch × 13/16 inch × 0.010 inch) which was completely taped with one layer of 0.003 inch H-film. One 0.010 inch dia. hole had been drilled through the Kapton insulator prior to its application on the conducting surface and this hole was placed at the center of the 3/8 inch × 13/16 inch rectangle. The sample was placed in the plasma wind tunnel and I_D vs. V_B measurements were taken. With a plasma density of $n_+ = 10^6$ ions/cm^3 and a streaming velocity of $v_+ = 16$ Km/sec the initial drainage current was 0.3 ma with the sample biased at $V_B = 800$ V. As time progressed the current collected diminished to 0.1 ma. The bias voltage was increased to 1100V where I_D increased to 0.3 ma. However, I_D again decreased to zero in a short time. When V_B was increased to 1500 volts the drainage current I_D held at 0.6 ma for a short while; however, within 20 minutes the drainage current increased to 2.0 ma. At this bias voltage and collection current, a faint glow at the conduction point could be seen. This test seems to indicate that the Kapton insulator, although effective at low power drains, can break down like the epoxy when enough power is concentrated in the conduction region.

A second sample identical in construction to Sample C_1 was also mounted in the plasma wind tunnel. This sample, C_2, was biased +3000 volts with respect to the tank wall and exposed to an argon plasma of density 1.2×10^5 ions/cm^3 and velocity 15.6 Km/sec for over 30 minutes. The leakage current remained approximately constant at about 0.1 ma during the time.

Following this initial exposure the ion density was increased to determine the effect of beam density on the leakage current. The results are presented in Table A. When the beam density was increased above 2×10^5 ions/cm^3 a discharge began between the exposed end of the 0.010 inch diameter Ta wire and the plasma. In order to prevent damage to the sample the bias voltage was immediately removed. The sample was kept at ground potential for a sufficiently long period of time (30 minutes) to permit the sample to dissipate any heat and cool to the ambient temperature. The plasma density was reduced and additional measurements were obtained which are shown in Table B. These measurements indicate increased drainage currents following the brief discharge.

The sample was biased +2000 V and exposed to a plasma of density of 1.4×10^5 ions/cm^3 for over 1 1/2 hours. Initially the leakage current was 170 μa. This increased slowly to about 220 μa after 1 1/2 hours with an average $\frac{\Delta I_D}{\Delta t} \leq \frac{0.5\ \mu\text{amps}}{\text{minute}}$. It had been previously noticed that with C_2 biased +2500 V and exposed to a plasma of density $n_+ = 1.84 \times 10^5$ ions/cm^3, and averaged over a shorter period of time, that $\frac{\Delta I_D}{\Delta t} \approx 10$ μamps/minute.

With Sample C_2 still biased +2000 V and $n_+ = 1.4 \times 10^5$ ions/cm^3 the local plasma potential was determined in the vicinity of the sample by means of an emissive probe. The sheath was found to extend about 12 cm from the sample both along the axis and perpendicular to the axis of the beam.

Examination of C_2 following these experiments showed that the exposed end to the Ta wire was slightly eroded and the epoxy was discolored.

TABLE A

Ion Density n_+ ($\times 10^5$ ions/cm^3)	Bias Voltage V_B (volts)	Drainage Current I_D (ma)
1.25	2500	0.08
1.25	3000	0.18
1.79	2500	0.20
1.84	2500	0.26
1.94	2500	0.30

TABLE B

Ion Density n_+ ($\times 10^5$ ions/cm^3)	Bias Voltage V_B (volts)	Drainage Current I_D (ma)
1.17	2000	0.13
1.09	2500	0.20
1.37	2000	0.17

IV. CDS SOLAR CELL TESTS PERFORMED IN THE PLASMA WIND TUNNEL

A one foot square CdS solar cell array was mounted on a 1/8 inch fiber glass board identical to the silicon solar cell support panel. All exposed tabs and conducting surfaces were covered by Kapton "H-film" tape and the panel was placed in the vacuum tank at the previous test position.

With the ion engine off (no plasma) the panel was biased up to 3000 volts with no leakage current observed. The panel was then exposed to an argon plasma $n_+ = 1.9 \times 10^5$ ions/cm^3 and $v_+ = 16$ Km/sec. With the panel biased +700 volts no drainage currents were observed initially. After about 5 minutes the drainage current was about 40 μamps which increased to 230 μamps after another 3 minutes. The bias was removed at this time and the plasma density reduced to 1.6×10^5 ions/cm^3. With a bias of +700 volts the leakage current increased from 36 μamps initially to 950 μamps in 10 minutes. See Fig. 20. The experiment was repeated with a bias of 600 volts on the solar cell panel a plasma density of 2×10^5 ions/cm^3. The results were the same. The plasma density was reduced to about 1.2×10^5 ions/cm^3 and the panel biased at 600, 700, 800, 900, and 1000 volts successively. Each bias voltage was maintained about 20 minutes with no growth of the leakage current observed at any bias level. The results are presented in Fig. 21. No leakage current was observed with a negative bias up to -300 volts.

Examination of the solar cells after these tests revealed a few small pinhole burns on the CdS protective covering. The H-film tape appeared undamaged. A further check on leakage through the H-film tape was obtained by covering a 5 inch square stainless steel sheet with one layer of the H-film tape and mounting this sample in the previous test position. No drainage current was observed with bias up to +900 V with a plasma density of 6×10^4 ions/cm^3.

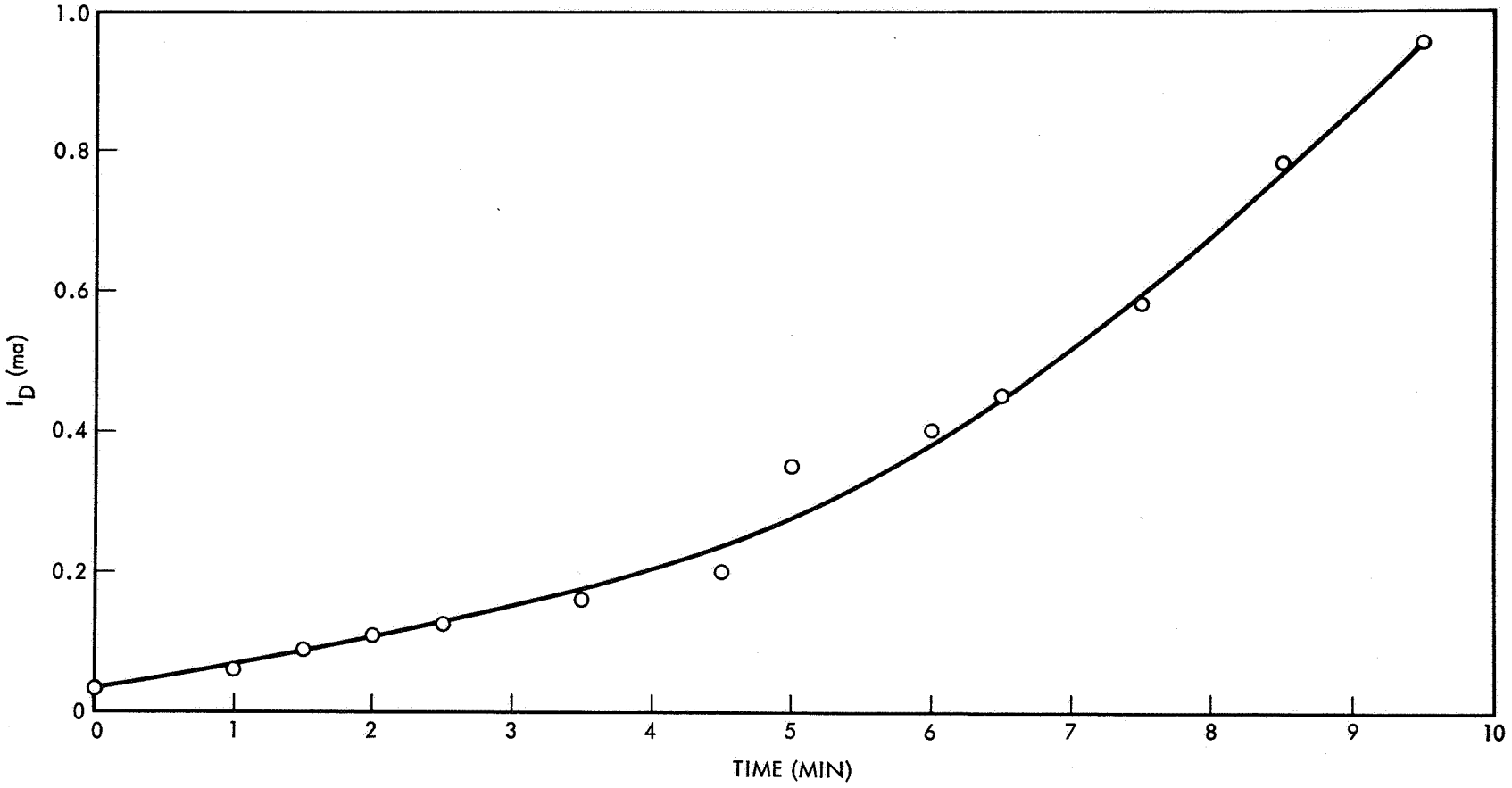

Figure 20. CdS solar cell drainage current (connecting tabs taped with 0.003 inch Kapton "H-film") as function of time. Pulsed argon plasma (50% duty cycle) $n_+ = 1.9 \times 10^5$ ions/cm^3, $v_+ = 16$ Km/sec and $V_B = +700$ volts.

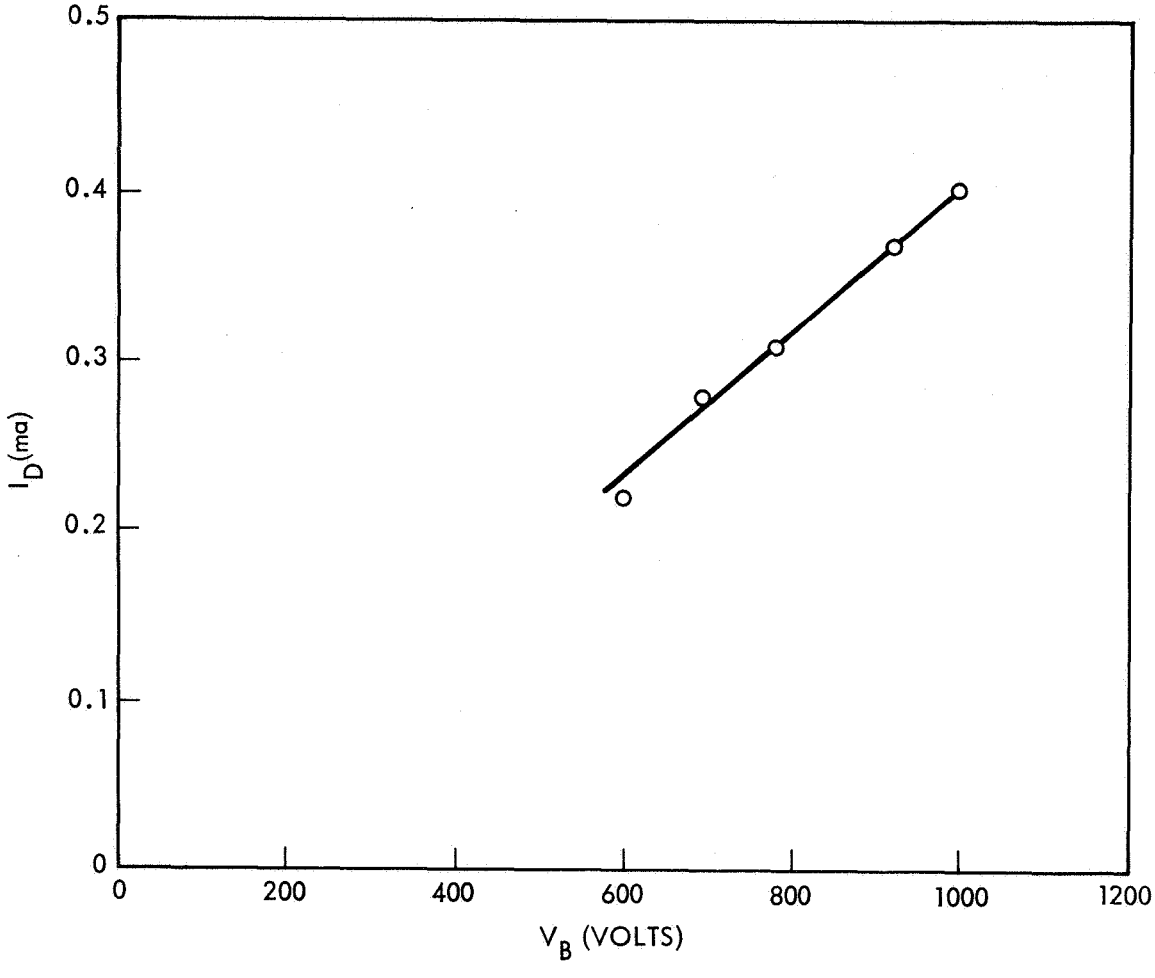

Fig. 21. CdS solar cell drainage current (connecting tabs taped with "H-film") as function of bias voltage. Pulsed argon plasma $n_+ = 1.2 \times 10^4$ ions/cm^3 and $v_+ = 16$ Km/sec. For this low density plasma I_D does not grow with time.

V. MAGNETIC FIELD EFFECTS

The experiments described in the previous sections were conducted in the presence of the earth's magnetic field. This magnetic field, in the testing chamber of the plasma wind tunnel, possesses a component perpendicular to the axis of the chamber of $\sim$ 0.35 gauss. Fields of this order of magnitude do not materially affect the properties of the plasma stream flow along the chamber axis. It was considered possible, however, that such transverse fields might affect the flow of electrons from the plasma stream to the positively biased drainage point. Magnetic field effects, usually of a suppressing nature, are expected in Langmuir probe applications wherever the electron radius of curvature in the magnetic field becomes comparable to the sheath dimensions. As will be discussed in the Appendix following, extensive sheaths have been noted for the experimental conditions utilized, and, particularly near the outer boundaries of the "bipolar" region, curvature of electrons by magnetic fields and accompanying effects on electron collection would be expected.

To test the magnitude of such B-field effects, Sample C_3 was placed in the plasma wind tunnel and a flow of 2×10^5 ions/cm^3 density at an ion streaming velocity of $\sim$ 16 kilometers/sec was generated. A potential bias of 880 volts was applied to the drainage point and the drainage current noted. The magnitude of transverse magnetic field initially present was 0.35 gauss. Removal of this transverse field through the activation of the chamber deguassing coils resulted in a 10% increase in the electron current collected. Application of current in the coils such as to double the transverse B-field (to 0.7 gauss) led to a 20% decrease in the collected current. Variations in collected current between 0 and $\sim$ .7 gauss transverse field thus yielded an overall variation of $\sim$ 30% in collected electron current.

Turning now to the operation of solar cell arrays in the near vicinity of the earth, one may note that the range from 0 to 0.7 guass encompasses the entirety of possible values of transverse magnetic fields. From the experiments above, one may conclude that the B-field variations do not alter in a substantive fashion, the findings, and data taken in the presence of the earth's B-field will be generally valid for all possible conditions of magnetic field in the near earth region.

For regions more distant from the earth, the magnetic fields diminish to very low values. For these regions the current collection would be enhanced over the laboratory data by amounts of the order of 10%. Such amounts cannot be considered to alter in any significant manner, the findings of these studies.

APPENDIX A

ELECTRON DRAINAGE IN STREAMING PLASMAS

The collection of charge carriers by a material body in a plasma has been treated extensively. A summary of much of this work is given by Chen[1]. The interpretation of the collected current and the functional dependence of this current on the potential difference between the material body and the plasma is, probably, the most commonly used method of diagnosis for the plasma state. However, this "Langmuir probe" analysis is largely restricted to plasma whose bulk velocities with respect to the material body are small compared to the thermal velocities of both the ions and the electrons. In particular, there are no adequate descriptions for the collection of electrons by highly positive probes immersed in high ion Mach number streaming plasmas. This is, however, the precise condition of electron drainage to small exposed points in highly positive solar cell arrays for spacecraft orbiting in the lower ionosphere or moving through the interplanetary regions. The experimentally observed behavior, utilizing plasma wind tunnels, has demonstrated that this overall plasma-material body configuration leads to a collection of electrons far in excess of that for similar probes and probe biasing potentials in stationary plasmas. The interest of this Appendix will be to evaluate the enhancement in the collection current between stationary and streaming plasmas and to discuss several possible contributing factors to this enhancement.

The electron current collected by a highly positive spherical probe in a stationary plasma is given in Chen[1] as

$$I_e = A_a j_r (1 + \eta)$$

where A_a is the probe area

j_r is electron current density diffusing to the sheath boundary,

and $\eta = \frac{eV_a}{kT_e}$ where V_a is probe potential

and T_e is electron temperature in the plasma.

The quantity j_r is given by $\frac{\rho_e \langle v_e \rangle}{4}$ where ρ_e is electron density in the plasma and $\langle v_e \rangle$ is the average electron thermal velocity in the plasma. the formula given above is valid is $\eta >> 1$. The theory from which it derives is drawn for collisionless plasmas. Orbital considerations have been taken into account in the derivation. Consider now the following considerations:

$$\rho_e = 1.6 \times 10^{-13} \text{ coulombs/cm}^3$$

$$\langle v_e \rangle = 4 \times 10^7 \text{ cm/sec}$$

$$A_a = 5 \times 10^{-4} \text{ cm}^2$$

$$V_a = 2500 \text{ volts}$$

The average electron thermal velocity given here corresponds to an electron temperature of $\sim$ 2500°K which approximates roughly the electron temperature in the plasma wind tunnel while the charge density of 1.6×10^{-13} coulombs/cm^3 (10^6 electrons/cm^3) also approximates that density encountered in the wind tunnel tests. For this example, $\eta \approx 10^4$ and

$$I_e = 8 \text{ } \mu\text{amps}$$

is the expected current to the probe for these conditions.

The result above may be compared to the current drain by positive probes whose initial collecting area was 5×10^{-4} cm^2, and which were immersed in <u>streaming</u> plasmas of 10^6 electrons/cm^3 at an electron temperature of $\sim$ 2500°K and for a probe bias potential (relative to the plasma) of 2500 volts. While the probe area is the same as that used in the spherical probe analysis the probe geometry is not spherical. Instead, the probe exposed surface is a disc whose diameter is .025 cm and which is set flush into an insulating surface as shown in Fig. 22. A first estimate of the behavior of this probe is that it would have a reduced collection relative to a spherical probe of

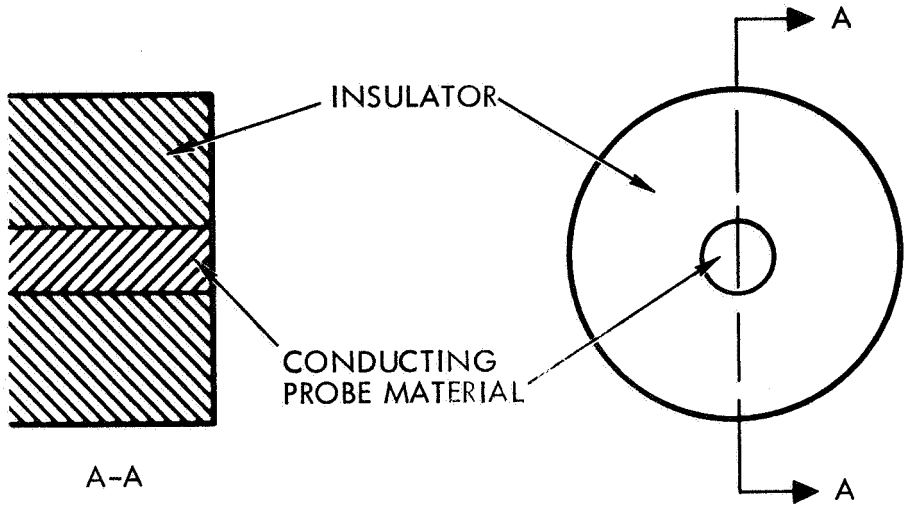

Figure 22. Diagram of conducting disc flush with, and surrounded by insulation material (disc probe).

the same area. There are two reasons to expect a reduced collection. First, the sheath for the spherical probe extends over a solid angle of 4π steradians about the probe. For the probe in Fig. 22, the sheath is confined to a solid angle of, at most, 2π steradians (the forward direction). The compression of electron trajectories into a smaller range of approach directions leads to higher space charge densities. These higher space charge densities cannot be supported over as large a radial extent as in the case of the spherical probe and, hence, the total sheath area connecting to the undisturbed plasma is reduced for the "disc" probe. A second factor which should reduce the collection of the disc relative to the spherical probe is the presence of insulating surfaces. Electrons whose orbits in the sheath lead to narrow misses of the probe surface have total dwell times near the probe of the order of nanoseconds or less for the spherical probe and thus have a limited period of prevention, by their space charge, against other electrons entering those regions of the sheath near the probe. For the disc probe, however, a near miss by an electron results in striking the insulating surface. The drainage time for such electrons is not known, but it must be considerably in excess of the nanosecond condition described earlier. It would be expected, then, that charge buildup on the insulating surface would result and that the space charge forces of this surface layer would reduce the current of electrons entering the sheath regions near the probe. Both of the discussed factors then should lead to disc probe currents which are reduced relative to the current to a spherical probe. The experimental evidence, however, was that disc probe currents far in excess of the 8 μampere figure were drawn.

The current drawn to the disc probes in streaming plasmas cannot be characterized by a single figure. For plasma densities of 10^6 electrons/cm^3 and probe potentials of 2500 volts, the initial probe current was, typically, about 100 μamperes. In time, however, the probe currents increased to levels of several milliamperes. Factors relating to this increase will be discussed in later paragraphs. The present discussion will consider the initial drainage situation during which probe surfaces and insulators are not ablated. For this initial condition, the probe collection would appear to be at least an order of magnitude in excess of that predicted for a stationary plasma. Evidence indicates that this enhancement is caused by the condition of a streaming plasma.

The sheath separating the probe from the undisturbed portions of the plasma stream is indicated schematically in Fig. 23. It should be emphasized that this representation is only schematic. Some details such as the extent of the sheath in particular directions have been experimentally determine, but the bulk of the description remains without direct experimental verification.

In this discussion it will be assumed that the sheath configuration is steady-state--that is, that its properties do not fluctuate in time. For certain plasma-sheath arrangements this steady-state behavior does not exist. In particular, for plasmas streaming against a planar material boundary at high positive potentials, oscillations in the sheath have been commonly observed. However, for sheaths in which a substantial "compression" of electron trajectories exist, (i.e. that the collection point for electrons has an area much less than the area of the sheath as it terminates on the plasma), the sheath is usually non-fluctuating in time. Such a condition of compression exists in the sheath illustrated in Fig. 23. Along some outer boundary (indicated by the dotted line) the electric fields are assumed to vanish. Outside of this boundary the electric field remains uniformly zero. An approximation is being made here, since very weak electric fields probably penetrate into the plasma for distances which are large compared to the dimensions indicated by the dotted line. However, the probing of the sheath by emissive probes has shown that observable electric fields are only to be found within $\sim$ 10 centimeters from the collection point, and, hence the assumption of zero electric field outside the indicated boundary is justified for this present treatment.

Since electric fields do vanish outside this boundary, ion trajectories for the streaming plasma are undisturbed. Inside the boundary, however, electric fields cause both ion and electron trajectories to alter and ion and electron energies to change. Ions are decelerated by the electric field and lose kinetic energy in their penetration of regions of elevated potential. Electrons are accelerated by the field to higher velocities, and their trajectories are compressed inward. This second region will be termed the "bi-polar" region in that charge carriers of both signs exist within it. At some inner boundary to this bipolar region, however, ion penetration ceases, and the

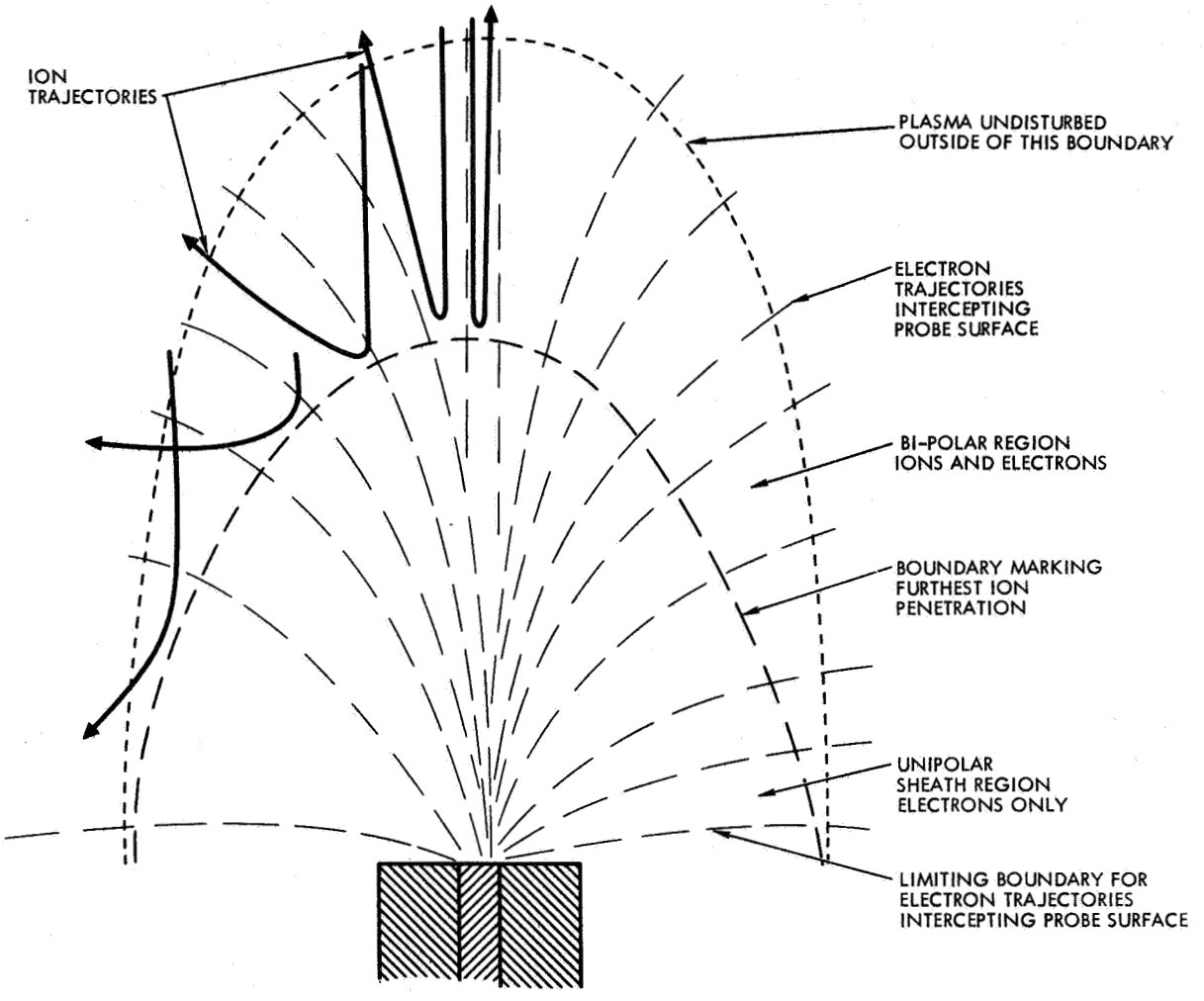

Figure 23. Schematic representation of sheath around "disc probe" for positive bias voltage applied to conducting element.

remaining portions of the sheath terminating at the electron collection point constitute a unipolar (electron) flow region. This boundary and the turnaround of ions at this boundary are indicated in Fig. 23 by the dashed line.

The dotted line marking the edge of the plasma sheath also denotes an equipotential in the plasma (since E vanishes everywhere along this boundary). The dashed line marking the termination of the bi-polar region is <u>not</u> an equipotential. This follows from the directed nature of the ion flow in streaming plasmas. For the ion which is directed along the axis of the drainage point sheath, the electric fields are precisely in opposition. Such an ion will be brought to rest (all velocities components zero) at its reflection point. This point also occurs for a potential equal to $\frac{M_+ v_o^2}{2e}$ where v_o is the ion velocity in the undisturbed plasma. For ions which impact on the sheath at points off the drainage point-sheath axis, the maximum penetration of the sheath does not result in the ion being brought to rest. Rahter, the ion at its reflection point possesses a non-zero velocity component, v_t, parallel to the dashed line, ion kinetic energy is non-zero, and the potential at the reflection point is given by $\frac{M_+}{2e}\left(v_o^2 - v_t^2\right)$. Now, for ions impacting on the sheath at larger distances from the drainage point-sheath axis, the remaining velocity at reflection grows larger, approaching v_o. Thus, for those regions at the greatest distance from the drainage point axis, the potential at the reflection point diminishes to V = 0 (the reference potential of the undisturbed plasma).

The electron behavior in the bi-polar region is that of acceleration and compression. The compression of electron trajectories causes an increase in electron current density in moving inward from the sheath boundary. Such an increase would, nominally, result in an increase in the electron charge density. However, the acceleration of the electrons by the field in the bi-polar region causes electron densities to decrease. Present information on the sheath does not permit a judgment on which of these two effects, charge density increase or decrease, predominates. The bi-polar region, moreover, is further complicated by the effects of ion motion. In being decelerated the space charge density of the ions is increased. This increase is further compounded because of the reflection of ions, so that

the ion current density must include both incoming and outgoing ion streams. The ion penetration of the sheath region is, perhaps, the crucial element in the observed behavior that electron collection for the streaming plasma is greatly enhanced over predictions based upon "stationary" plasma. Because of the penetration, slowing and reflection of the ions, ion density is increased and charge neutralization of even enhanced electron densities is provided. Furthermore, the electric fields in the bi-polar regions provide for acceleration of electrons, diminution of electron space charge density and the eventual injection of these now accelerated electrons into the final "unipolar" region.

The extent of electron acceleration prior to entry in the unipolar region depends upon $\frac{M_+ v_o^2}{2}$, the ion streaming energy in the undisturbed plasma stream. For spacecraft orbiting in the lower ionosphere, the apparent ion streaming energy may be as high as 20 electron volts. For this situation, the electron injection into the unipolar region of the sheath can occur with electron energies of up to 20 electron volts. If the electrons in the undisturbed plasma possessed 0.2 electron volts, the bi-polar region acceleration of electron velocities is a factor of 10, thus allowing a compression of electron current density by a factor of 10 with no increase in electron space charge density. For spacecraft orbiting at higher altitudes, the diminution of the ion mass leads to greatly reduced apparent ion streaming energies. However, for still further increases in altitude and for entry into the interplanetary plasma, the ion streaming energy becomes that of the solar wind and may range from hundreds of electron volts to thousands of electron volts. Thus, ion penetration effects may be expected to play a major role in electron collection from plasmas encountered in the lower ionosphere and in the interplanetary regions.

The unipolar region in Fig. 23 constitutes the final region of passage for the electrons in moving from the plasma to the drainage point. Here, both compression and acceleration occur. Because the drainage point is itself of such limited area, and since electron velocity proceeds only with a square root of electron acceleration energy, compression effects must dominate, and increasingly dense electron flows result in moving

toward the drainage point. This is the nominal behavior in any sheath. The distinction for this situation is that electrons are injected into the unipolar region with energies that may greatly exceed their energy in the undisturbed plasma and that electron collection from an extensive region of the undisturbed plasma is facilitated by the ion space charge neutralization in the bi-polar region.

To this point the discussion has considered only the plasma, the sheath regions, and the final drainage point. In the experiments, however, the probe consisted not only of the exposed conducting point but also of surrounding insulators. Both the conducting material and the insulators may be affected by the collection of the current. Two effects are of interest here. The first is the accumulation of electrons on insulating surfaces. From orbital considerations, many electrons in the sheath should be accelerated toward the drainage point yet, because of angular momenta, would miss the conducting material and strike the adjoining insulating material. This buildup of charge on the insulators should set up space charge fields which, in turn, should inhibit the flow of electrons into the exposed conducting area. The equilibrium build-up would also be governed by the rate at which charge can be drained away, presumably to the conducting element. For "good" insulators such drainage should be small compared to the current going to the collecting point. However, both the insulating and conducting materials can change their properties under the impact of the electrons. This constitutes the second of the two effects of concern. If one examines the current collected, in the earlier example, at 2500 volts probe potential, an initial value of 0.1 milliamperes was typical. The power input from this current is .25 watts. The probe area is 5×10^{-4} cm^2 leading to a power density at the probe surface of 500 watts/cm^2. Some of this power may be conducted away from the surface. However, even if a significant fraction of the heat may be conducted to other regions of lesser temperature, the remainder is sufficient to bring even the refractory materials up to the vaporization point. Finally, heat released into the surrounding insulating material may cause this material to deteriorate.

Two possible further processes may occur if the power input to the probe and the surrounding insulator is sufficiently high. The first of these is that vaporization of the probe surface could occur and that conducting material from the probe would deposit over the nearby insulator. The film of such redeposited material would connect with the now altered probe surface and together with that remaining probe surface would constitute a greatly expanded area for the collection of electrons. This expanded collecting area leads, in turn, to further increases in input power, to material destruction and to possible breakdown conditions. In examining probe surfaces it is apparent that this process has taken place on some occasions. A second possible process by which increased drainage currents are obtained is the erosion of the nearby insulator. As the insulating material withdraws, increased conducting area is exposed, and increased electron collection is obtained. Upon occasion, this second process has been observed. For both of these processes there are additional possible effects. These effects arise if ionization of the evaporating material from the probe surface and insulators can occur with sufficient intensity.

In the previous discussion it was assumed that the region immediately in contact with the probe surface was a unipolar region (electrons only). However, electrons in the sheath are energetic and atoms of material evaporating from the probe and insulators must traverse this sheath region. If the atom becomes ionized, the most likely region must be in the unipolar region where high electron energies are encountered. The ionization results in an ion-electron pair, the electron of which moves rapidly away toward the probe, while the ion is accelerated outward toward the plasma. However, the ion mass very greatly exceeds the electron mass, and, thus, the ion remains in the sheath region for times which are long compared to the transit time of an electron across the sheath. During this comparatively long transit time, the ion provides a charge neutralization point for electrons. The exact effect of this extra charge neutralization in the "unipolar" region is difficult to determine, but a likely estimate is that for every ion formed in the sheath an additional number of electrons $= \sqrt{\frac{M_+}{m}}$

are allowed to move to the probe surface. An increased current of electrons leading to further atom evaporation, further atom evaporation, further ionization in the sheath, and still further electron collection would yield ultimately a "breakdown" condition. Upon occasion, it is felt that this is what has been observed. Small, but intense sources of light in the immediate neighborhood of the source demonstrate that excitation certainly exists and ionization is likely. It remains to demonstrate that the neutral material being excited and (possibly) ionized is material from the probe and insulating surfaces. Another possible source of background gas is the normal chamber gas during plasma wind tunnel operation. Spectral analysis of the light might confirm the source of the material under excitation and ionization, but such analysis was not possible during the tests under present discussion. However, in view of the amount of material removed from the probe and the surrounding insulator, it is likely that local neutral density is primarily from this ablating material and not the background chamber gas. An estimate is that local pressures of ablating material are at least three orders of magnitude above the local pressure of background (plasma wind tunnel) gas.

The discussion has, thus far, reviewed all the presently discernible processes that contribute to electron collection by exposed surfaces at high positive potentials. In particular, ion penetration into the sheath provides a charge neutralization for a region in which electrons are collected over broad areas and accelerated and compressed before injection into the area immediately adjacent to the probe. The increase in the collected current because of this "assistance" from ion penetration may be the greater part of the "order of magnitude" excess which exists for the streaming plasma case when compared to stationary plasmas. Because the collection is enhanced, the power input to the probe surface is enhanced and evaporation of the conducting material and/or ablation of the surrounding insulating material becomes possible. Such deterioration, when it occurs leads to even further enhancements in collected current, and, ultimately, breakdown conditions. Finally, there are occasions in which excitation and ionization of (probably) evaporating probe material leads to further charge neutralization of the electron flow and further increases in the allowed drainage current of electrons.

REFERENCES

1. Chen, Francis F., "Electric Probes," Plasma Diagnostic Techniques, edited by Richard H. Huddlestone and Stanley L. Leonard. Academic Press, New York, London, pp. 113-200 (1965).

OPERATION OF SOLAR CELL ARRAYS IN DILUTE STREAMING PLASMAS

by Robert K. Cole, H. S. Ogawa, and J. M. Sellen, Jr.

ABSTRACT

The operation of solar cell arrays in dilute streaming plasmas has been examined. Electron drainage currents from the plasma to exposed points in the cell array have been determined for cell bias potentials from 0 to 3000 volts positive with respect to the plasma for plasma densities ranging from 10^4 ions/cm^3 to 10^6 ions/cm^3. Argon ions were utilized in the streaming plasmas. Ion streaming velocities in the plasma wind tunnel ranged from 16 to 50 kilometers/second. Drainage currents from the plasma to reference drainage points with "pinhole" geometries and "slit" geometries were also determined. Effects of ambient magnetic fields upon electron drainages were examined.

REPORT DISTRIBUTION LIST FOR
CONTRACT NO. NAS3-10612

National Aeronautics and Space Administration
Washington, D. C. 20546
Attention: RNW/Arvin H. Smith
RN/William H. Woodward

National Aeronautics and Space Administration
Scientific and Technical Information Facility
P.O. Box 33
College Park, Maryland 20740
Attention: Acquisition Branch (SQR-34-54)

National Aeronautics and Space Administration
Goddard Space Flight Center
Greenbelt, Maryland 20771
Attention: W. R. Cherry

National Aeronautics and Space Administration
Lewis Research Center
21000 Brookpark Road
Cleveland, Ohio 44135
Attention: J. E. Dilley, MS 500-309
A. F. Forestieri, MS 500-201
B. Lubarsky, MS 500-201
D. T. Bernatowicz, MS 500-201
T. M. Klucher, MS 500-201
(9 + 1 reproducible)
N. D. Spakowski, MS 302-1
Library, MS 3-7
Report Control Office MS 5-1
Technology Utilization Office, MS 3-19
V. F. Hlavin, MS 3-14
H. Mark, MS 301-1
J. R. Jack, MS 301-1
N. T. Grier, MS 301-1
C. C. Conger, MS 54-1
S. G. Jones, MS 54-3
L. Rosenblum, MS 302-1

National Aeronautics and Space Administration
Electronics Research Center
575 Technology Square
Cambridge, Massachusetts 02139
Building 575, Room 500
Attention: Dr. Francis C. Schwarz

National Aeronautics and Space Administration
Manned Spacecraft Center
Houston, Texas 77058
Attention: A. E. Potter

Jet Propulsion Laboratory
4800 Oak Grove Drive
Pasadena, California 91103
Attention: Don W. Ritchie

Institute for Defense Analyses
Science and Technology Division
400 Army Navy Drive
Arlington, Virginia 22202
Attention: R. C. Hamilton

Prof, W. R. Mickelsen
Engineering Center
Colorado State University
Fort Collins, Colorado 80521

Flight Accessories Aeronautics Systems Division
Wright-Patterson AF Base, Ohio 45433
Attention: Joe Wise/Code APIP-2

Heliotek Corporation
12500 Radstone Avenue
Sylmar, California 74820
Attention: Eugene Ralph

Martin Company
Orlando, Florida 32805
Attention: Library

North American Aviation, Inc.
Autonetics Division
Anaheim, California 92805
Attention: P. R. August

Philco Corporation
Blue Bell, Pennsylvania 19422
Attention: Mr. A. E. Mace

RCA Laboratories
Princeton, New Jersey 08540
Attention: Paul Rappaport

Massachusetts Institute of Technology
Lincoln Laboratory
Lexington, Massachusets 02139
Attention: Dr. A. G. Stanley, Room D-025

Hughes Aircraft Corporation
Space Systems Division
P.O. Box 90919, Airport Station
Los Angeles, California 90009
Attention: Preston DuPont

TRW Systems
Electric Power Lab
One Space Park
Redondo Beach, California 90278
Attention: W. Luft

Boeing Company
P.O. Box 3707
Seattle, Washington 98124
Attention: H. Oman

Communications Satellite Corporation
2100 L. Street, N. W.
Washington, D. C. 20837
Attention: Denis J. Curtin

Navy Space Systems Activity
Air Force Unit Post Office
Los Angeles, California 90045
Attention: Richard Silverman

Lockheed Missiles & Space Company
P.O. Box 504
Dept. 58-30
Sunnyvale, California 94088
Attention: S. H. Lee, Building 538

Goodyear Aerospace Corporation
1210 Massillon Road
Akron, Ohio 44315
Attention: Richard Hose

Lockheed
6201 East Randolph Street
Los Angeles, California 90022
Attention: Ken Ray

McDonnell Douglas Corporation
Missile & Space Systems Division
3000 Ocean Park Boulevard
Santa Monica, California 90406
Attention: Howard Weiner

Martin-Marietta Corporation
Electronics Research & Development
P.O. Box 179
Denver, Colorado 80201
Attention: John H. Martin